Extreme Weather Events Originating from Interactions between Tropopause Polar Vortices and the North Atlantic Jet Stream

Kevin A. Biernat, Lance F. Bosart, and Daniel Keyser

Department of Atmospheric and Environmental Sciences

University at Albany, SUNY

41st Annual Northeastern Storm Conference

6 March 2016

Research support provided by NSF Grant AGS-1355960

kbiernat@albany.edu

What are Tropopause Polar Vortices (TPVs)?

- TPVs are defined as tropopause-based vortices of high-latitude origin and are material features (Pyle et al. 2004; Cavallo and Hakim 2009, 2010)

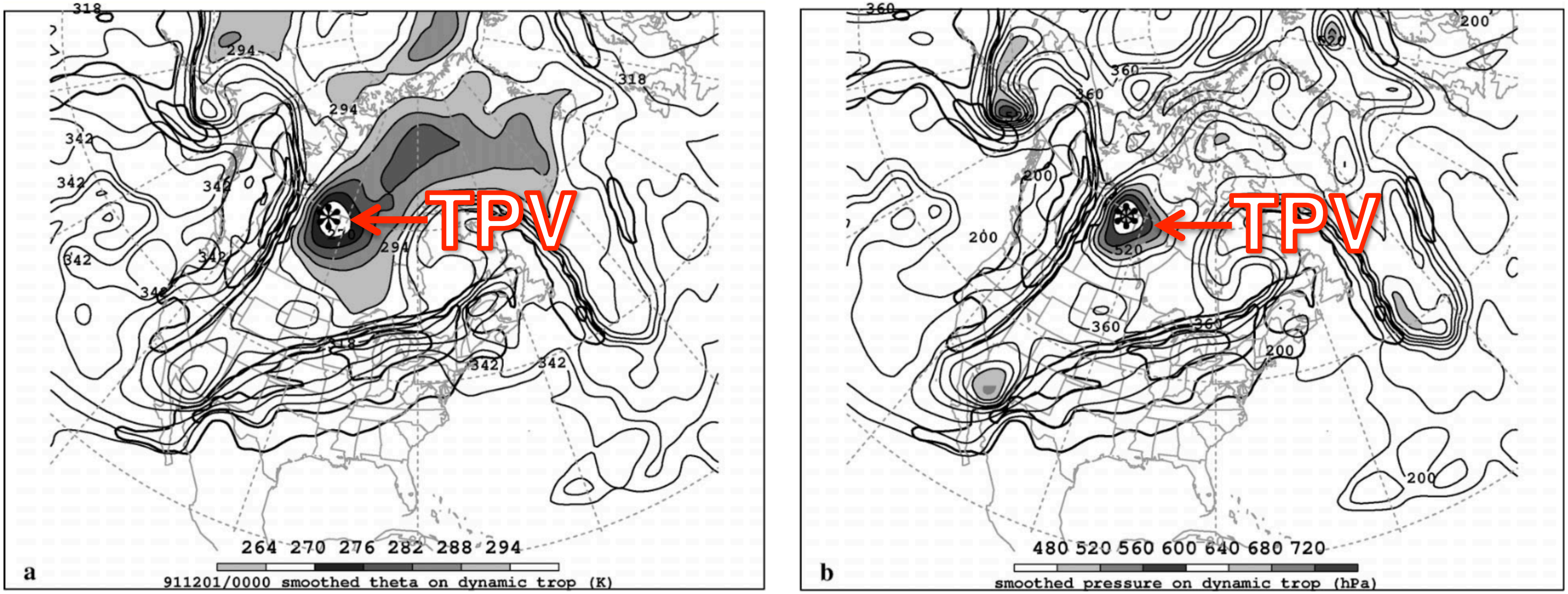

(left) Dynamic tropopause (DT) wind speed (every 15 m s^{-1} starting at 50 m s^{-1}, thick contours) and DT potential temperature (K, thin contours and shading) on 1.5-PVU surface valid 0000 UTC 1 Dec 1991; (right) same as left except DT pressure (hPa, thin contours and shading).
Adapted from Fig. 11 in Pyle et al. (2004).

Motivation

- TPVs may interact with and strengthen midlatitude jet streams, and act as precursors to intense midlatitude cyclogenesis events

Motivation

- TPVs may interact with and strengthen midlatitude jet streams, and act as precursors to intense midlatitude cyclogenesis events

- Interactions between TPVs and North Atlantic jet stream (NAJ) may lead to development of extreme weather events (EWEs) between North America and Europe

Outline

- Data and Methodology
- Case Study of 18–19 November 2013 extreme flooding event over Sardinia, Italy
- Conclusions

Data and Methodology

- 0.5° NCEP CFSR (Saha et al. 2010)
- Subjective TPV identification and tracking
  - TPV must be a coherent vortex that exhibits a local minimum of DT θ (i.e., closed contours of DT θ)
  - The vortex must be of high-latitude origin and last $\geq$ 2 days, similar to Cavallo and Hakim (2009)
  - Stop tracking TPV when it becomes significantly deformed during interaction with NAJ

18–19 November 2013 Sardinia Flood Event

- Slow-moving cutoff cyclone over Mediterranean leads to significant rainfall and flooding over portions of Sardinia
- Up to 467 mm of rain reported
- 16 deaths (Munich RE, 2014)
- Overall losses: ~780 million USD (Munich RE, 2014)

(Source: Google Maps)

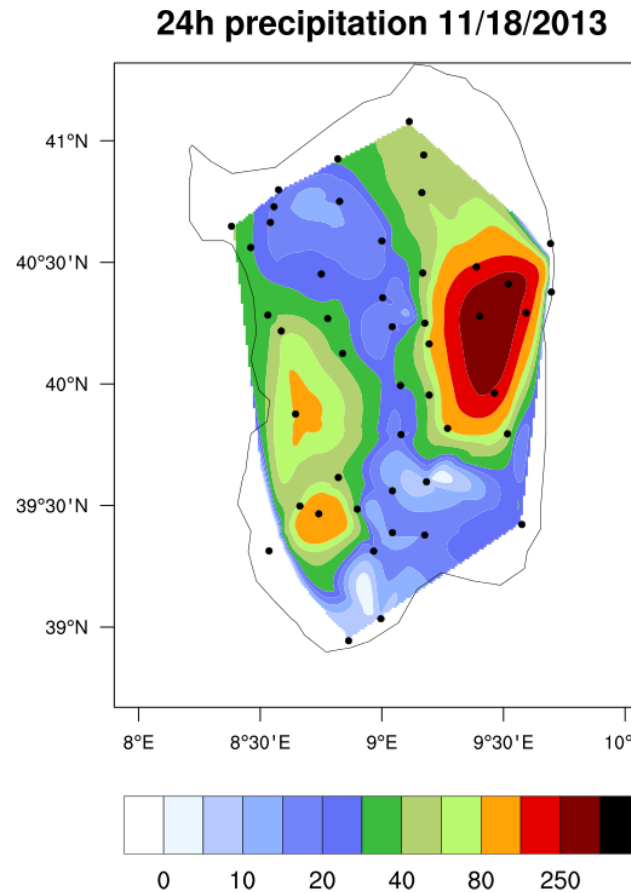

24-h accumulated precipitation (mm, shaded) during 18 Nov 2013 (Source: Julian Quinting)

TPV Track: 1800 UTC 6 Nov – 0000 UTC 14 Nov 2013

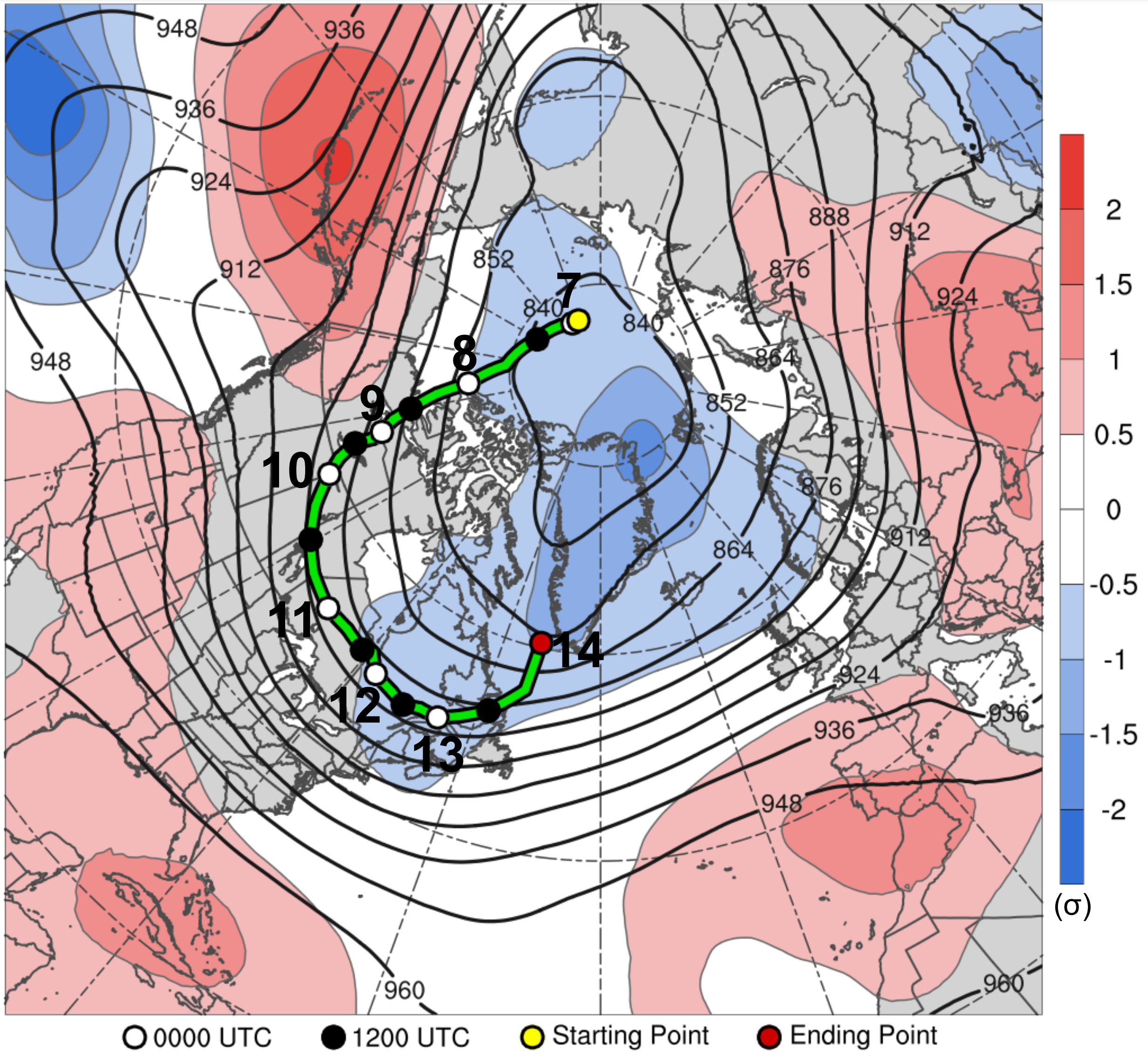

6–14 Nov 2013 time-mean 300-hPa geopotential height (dam, black) and standardized anomaly of geopotential height (σ, shaded)

TPV Extraction

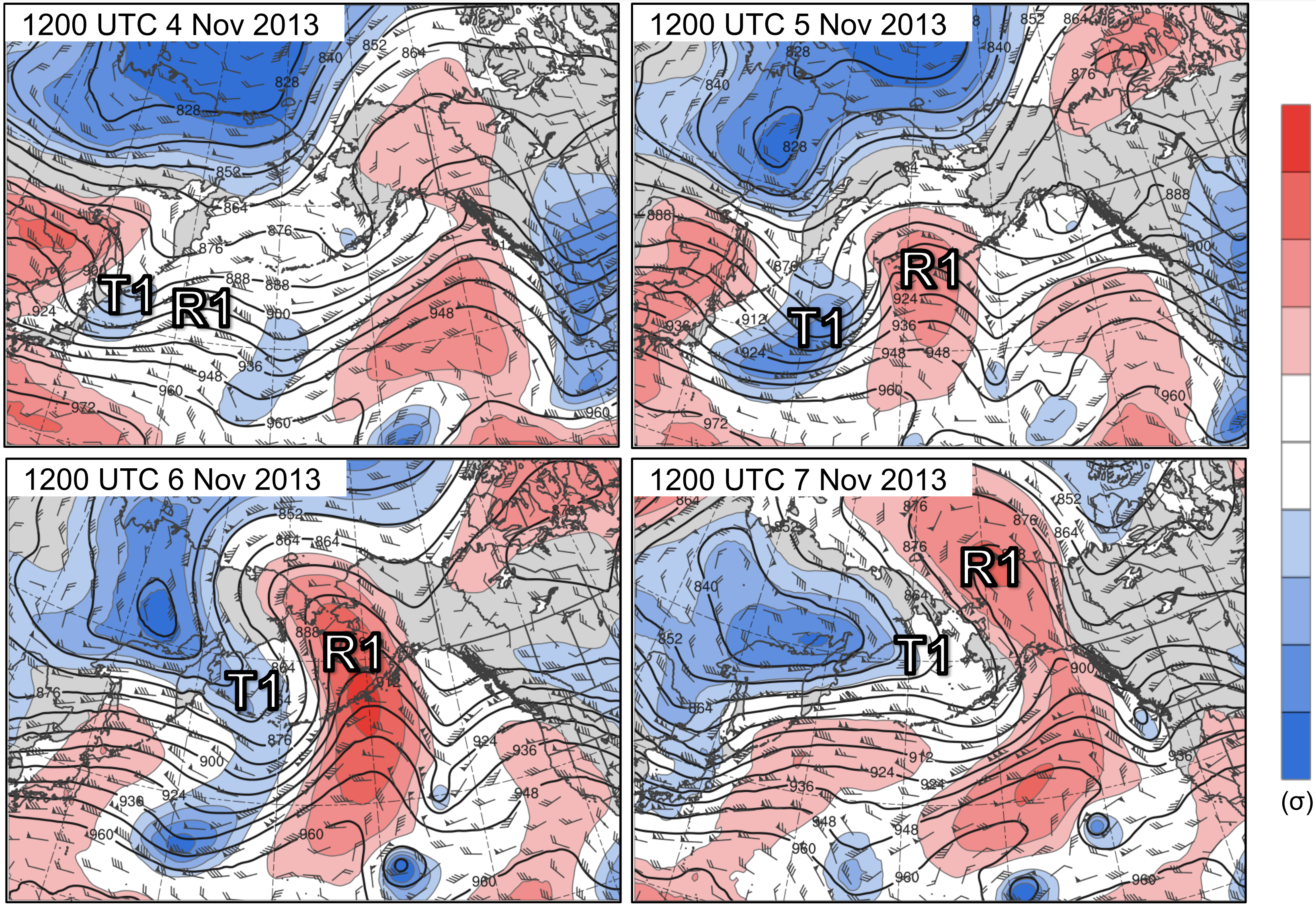

300-hPa geopotential height (dam, black), wind (m s^{-1}, barbs), and standardized anomaly of geopotential height (σ, shaded)

TPV Extraction

1200 UTC 4 Nov 2013

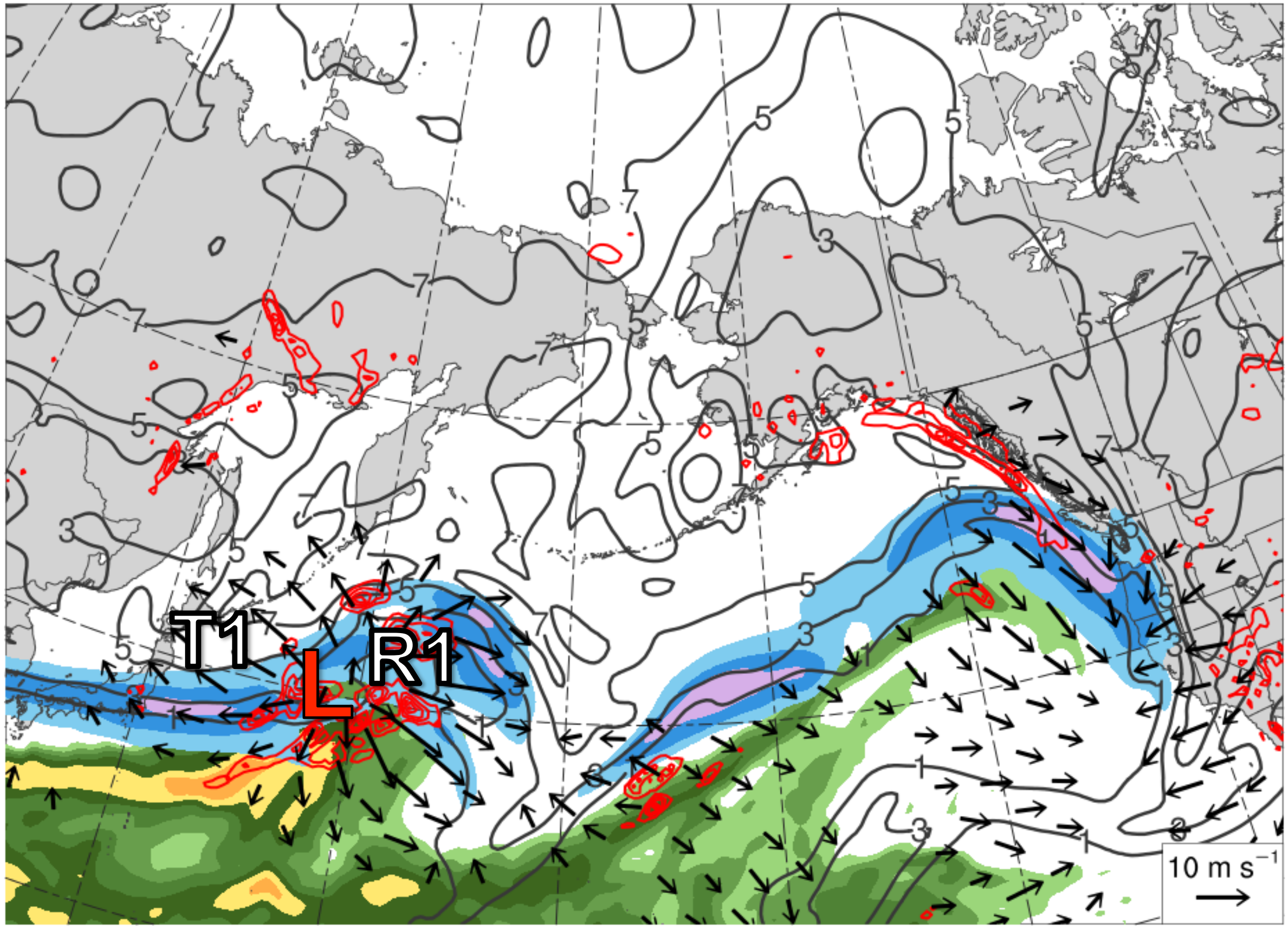

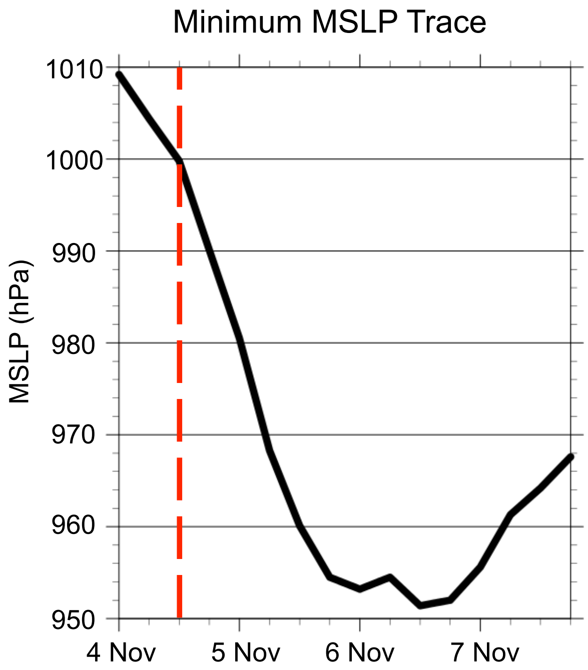

300–200-hPa PV (PVU, gray) and irrot. wind (m s^{-1}, vectors), 250-hPa wind speed (m s^{-1}, shaded), 600–400-hPa ascent (every 0.5 × 10^{-3} hPa s^{-1}, red), PW (mm, shaded)

TPV Extraction

1200 UTC 5 Nov 2013

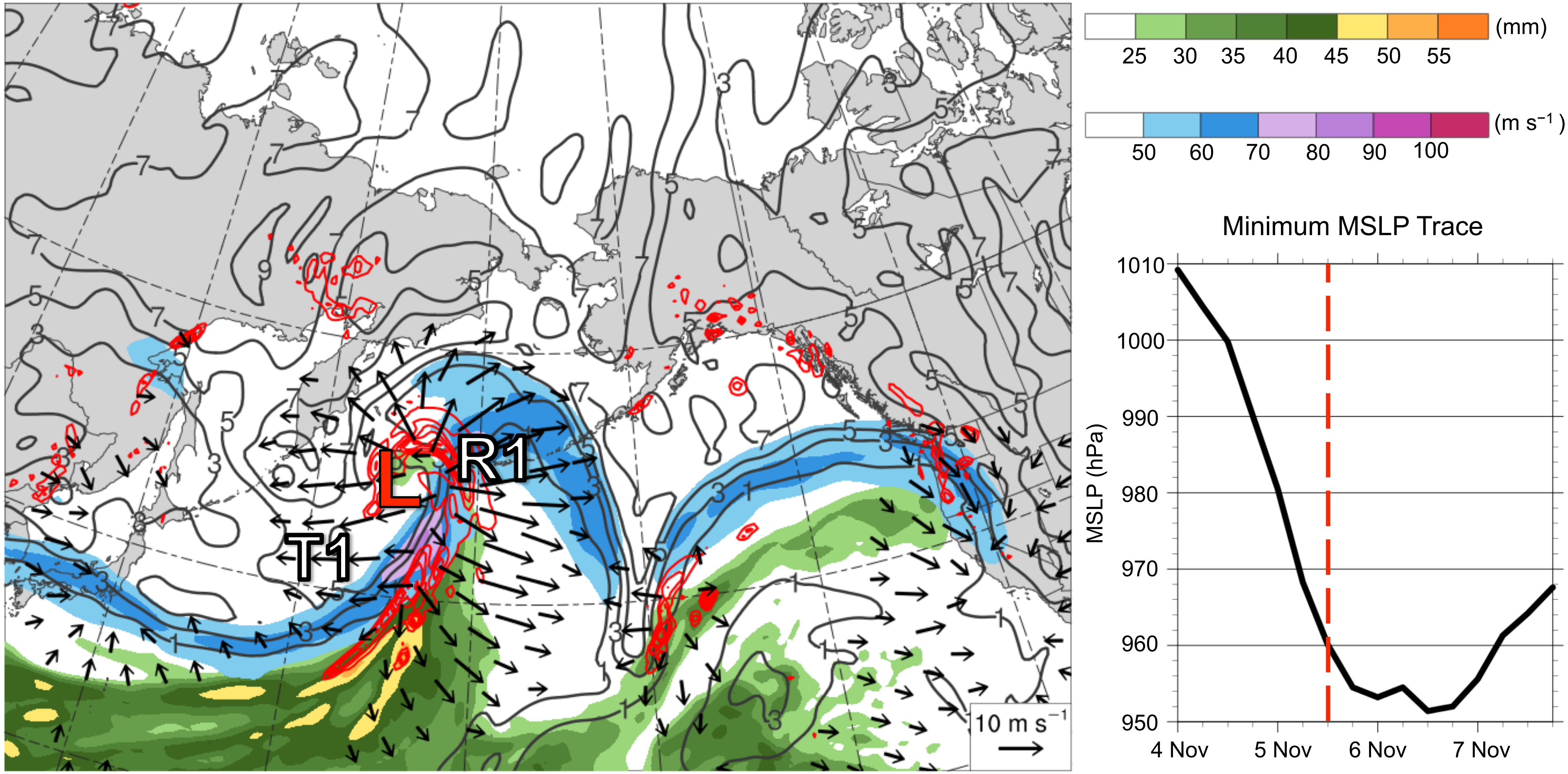

300–200-hPa PV (PVU, gray) and irrot. wind (m s^{-1}, vectors), 250-hPa wind speed (m s^{-1}, shaded), 600–400-hPa ascent (every 0.5 × 10^{-3} hPa s^{-1}, red), PW (mm, shaded)

TPV Extraction

1200 UTC 6 Nov 2013

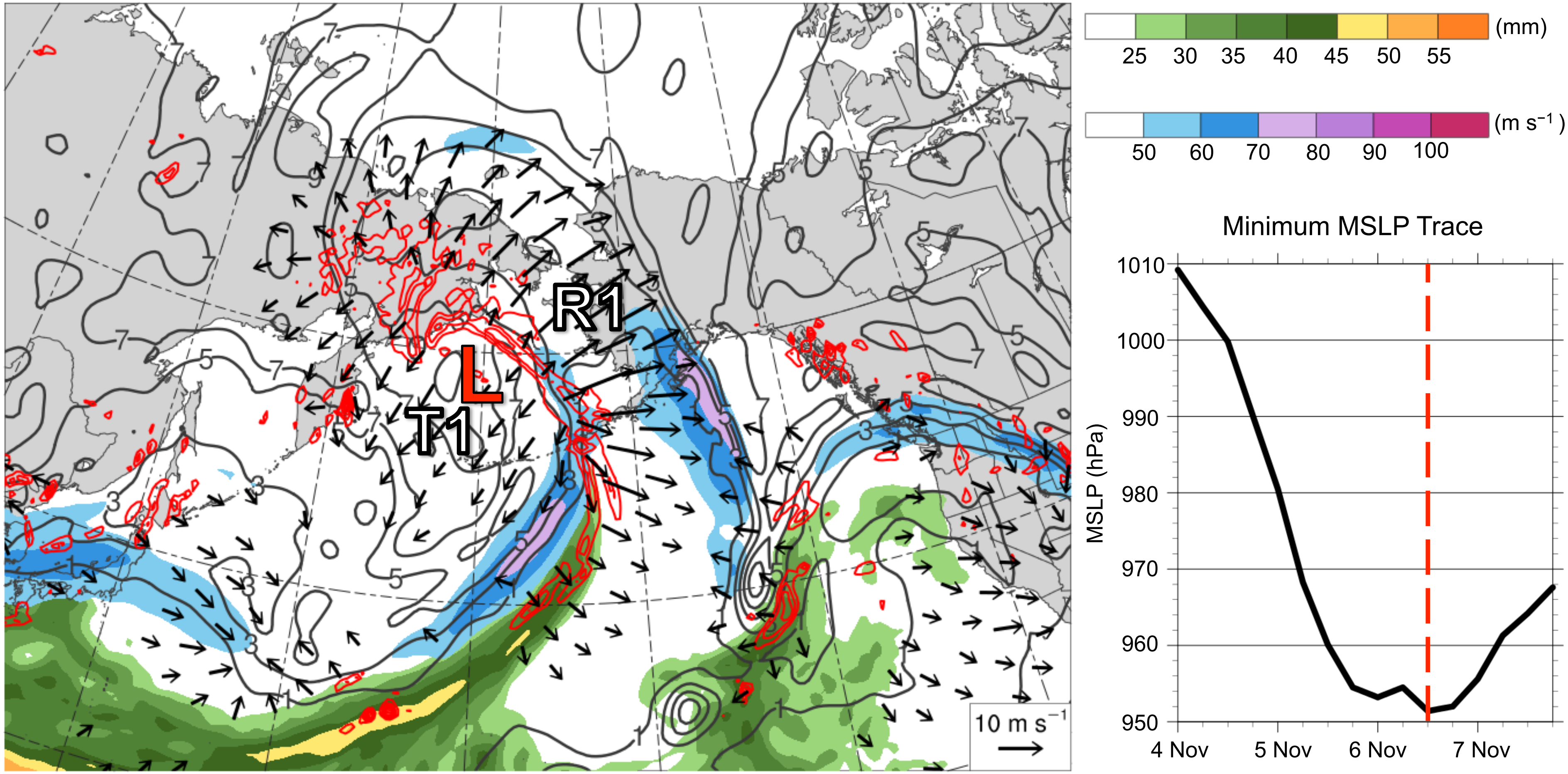

300–200-hPa PV (PVU, gray) and irrot. wind (m s^{-1}, vectors), 250-hPa wind speed (m s^{-1}, shaded), 600–400-hPa ascent (every 0.5 × 10^{-3} hPa s^{-1}, red), PW (mm, shaded)

TPV Extraction

1200 UTC 7 Nov 2013

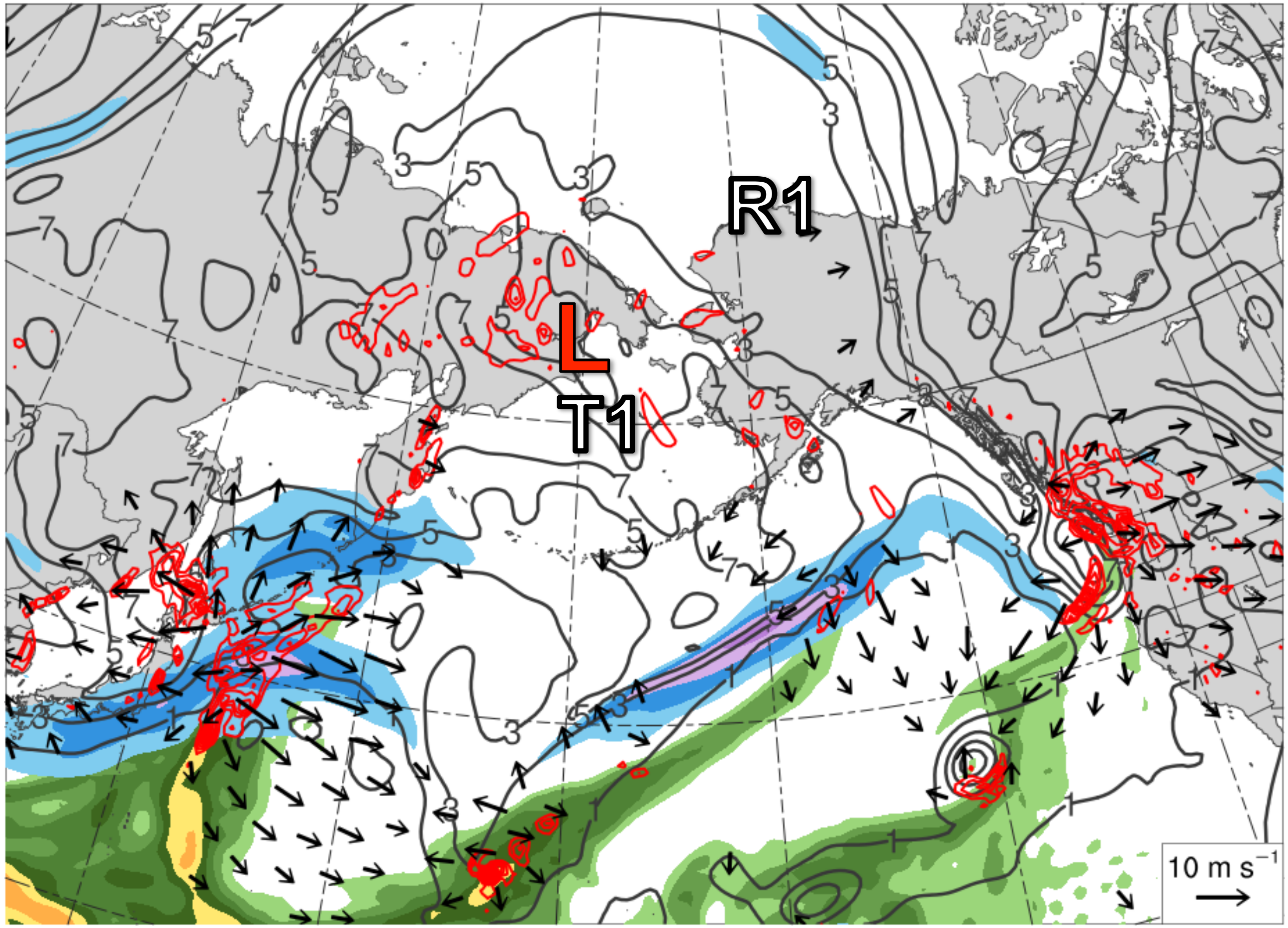

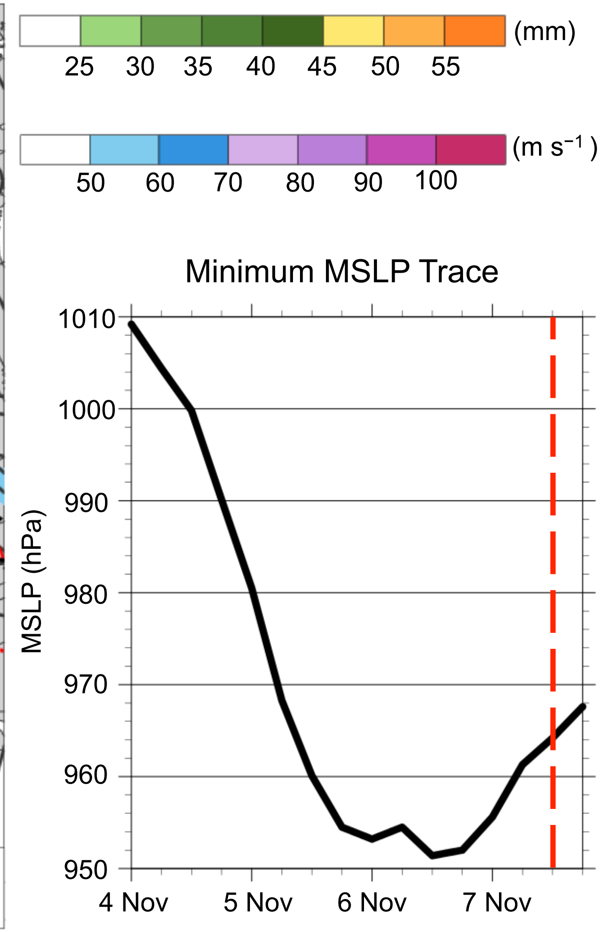

300–200-hPa PV (PVU, gray) and irrot. wind (m s^{-1}, vectors), 250-hPa wind speed (m s^{-1}, shaded), 600–400-hPa ascent (every 0.5 × 10^{-3} hPa s^{-1}, red), PW (mm, shaded)

TPV Extraction

1200 UTC 7 Nov 2013

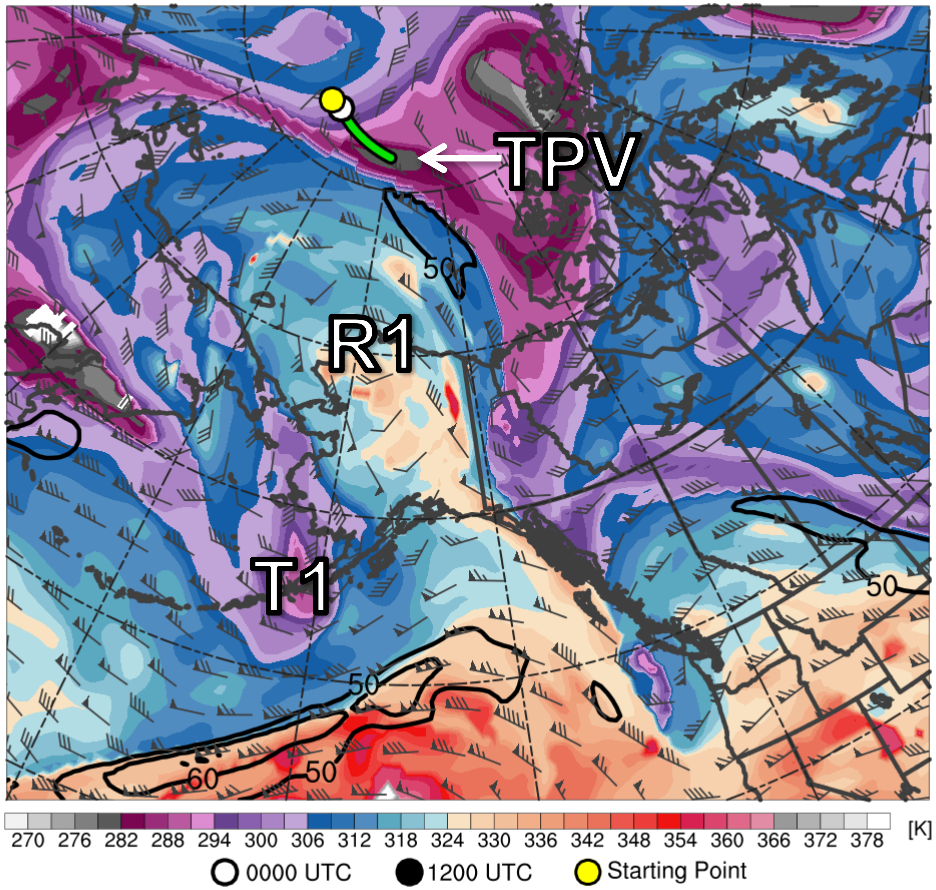

Potential temperature (K, shaded), wind speed (black, every 10 m s^{-1} starting at 50 m s^{-1}), and wind (m s^{-1}, barbs) on 2-PVU surface

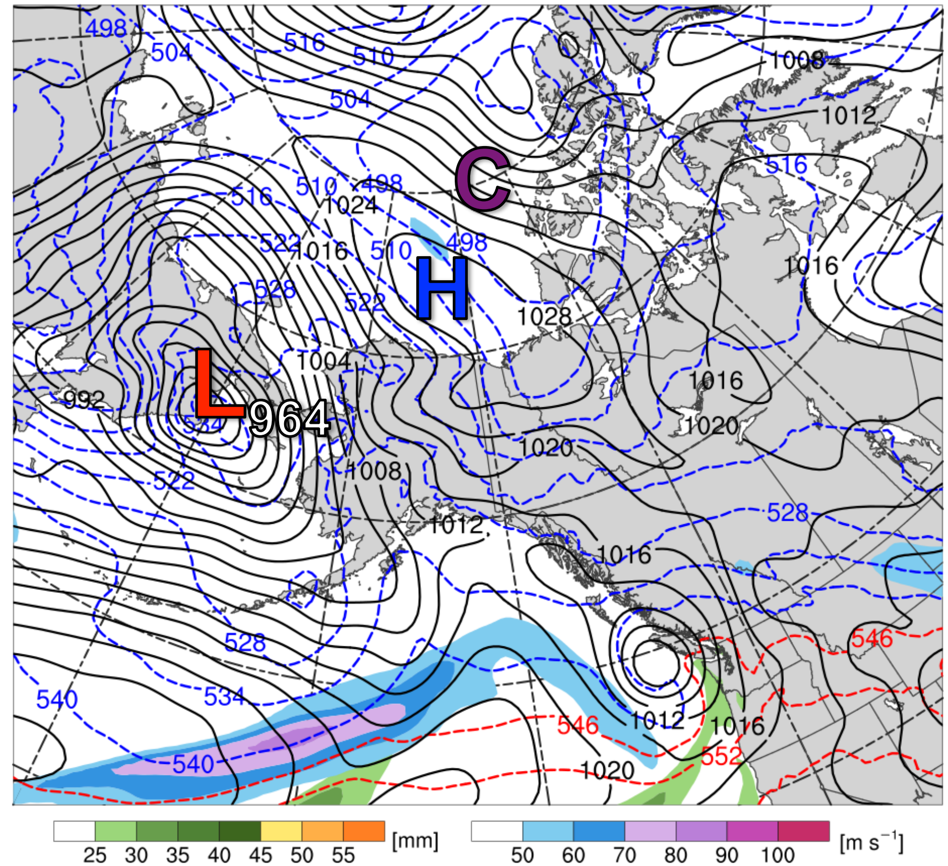

250-hPa wind speed (m s^{-1}, shaded), 1000–500-hPa thickness (dam, blue/red), MSLP (hPa, black), PW (mm, shaded)

TPV Extraction

1200 UTC 9 Nov 2013

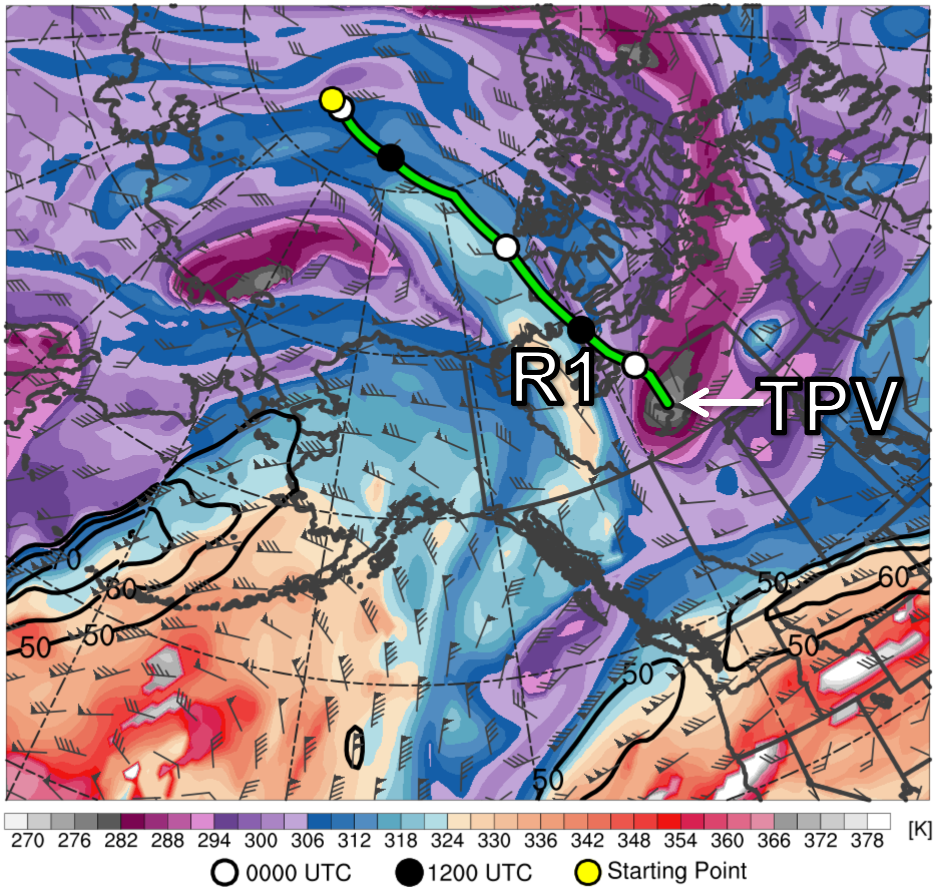

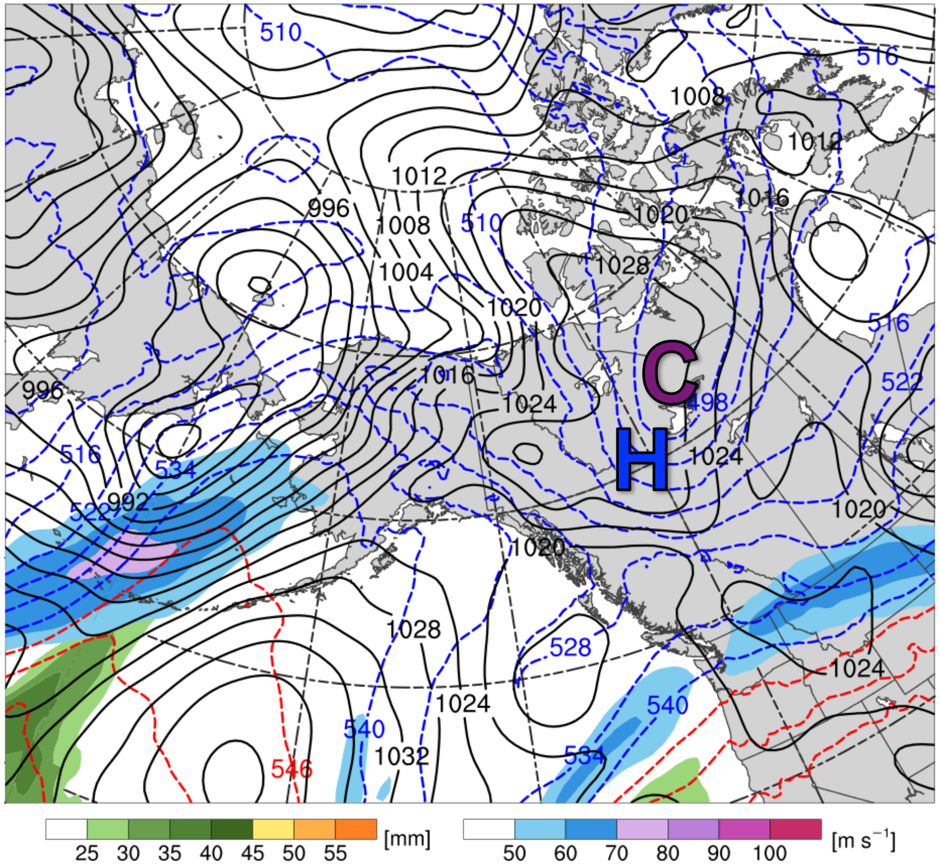

Potential temperature (K, shaded), wind speed (black, every 10 m s^{-1} starting at 50 m s^{-1}), and wind (m s^{-1}, barbs) on 2-PVU surface

250-hPa wind speed (m s^{-1}, shaded), 1000–500-hPa thickness (dam, blue/red), MSLP (hPa, black), PW (mm, shaded)

TPV–NAJ Interaction

1200 UTC 11 Nov 2013

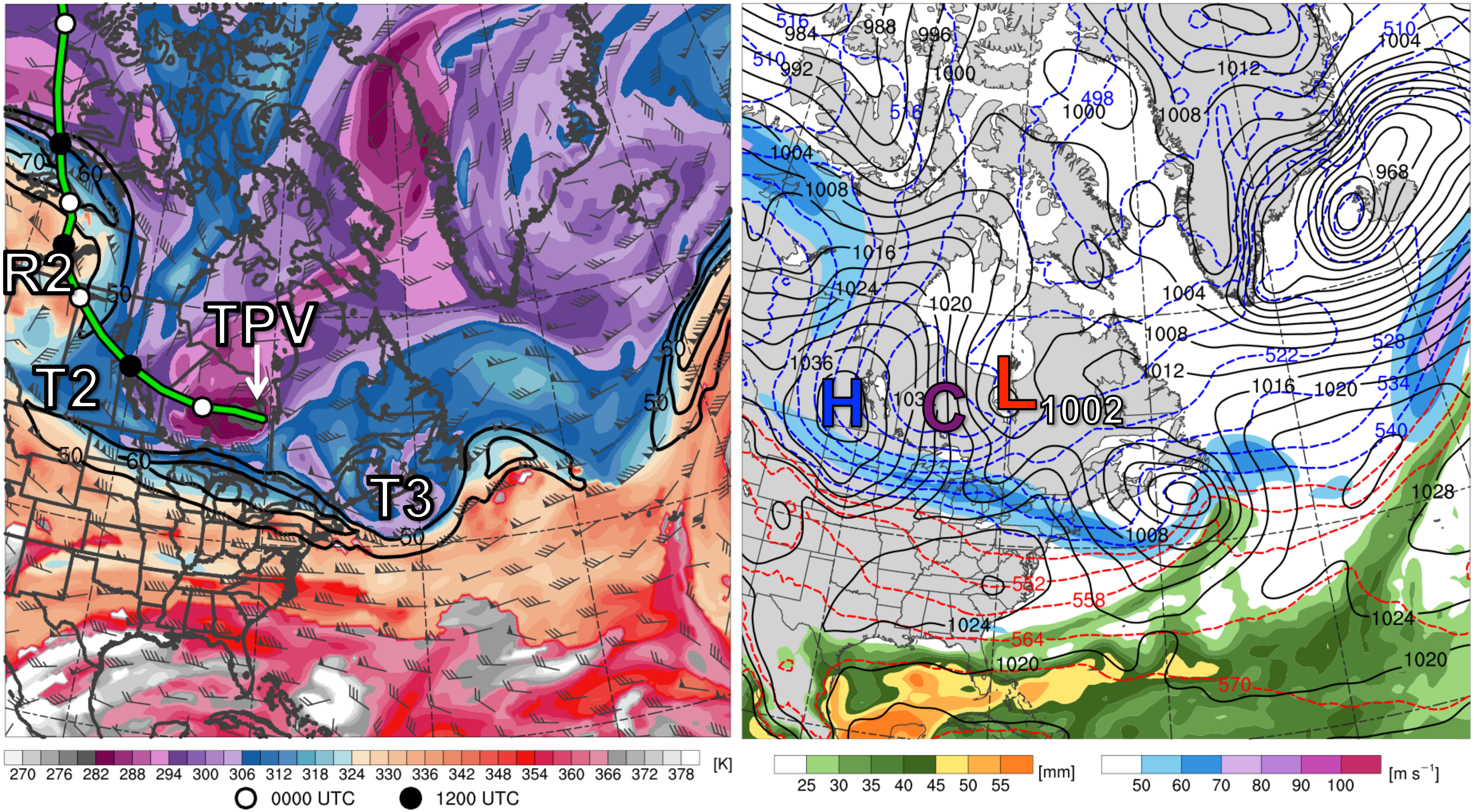

Potential temperature (K, shaded), wind speed (black, every 10 m s^{-1} starting at 50 m s^{-1}), and wind (m s^{-1}, barbs) on 2-PVU surface	250-hPa wind speed (m s^{-1}, shaded), 1000–500-hPa thickness (dam, blue/red), MSLP (hPa, black), PW (mm, shaded)

TPV–NAJ Interaction

0000 UTC 12 Nov 2013

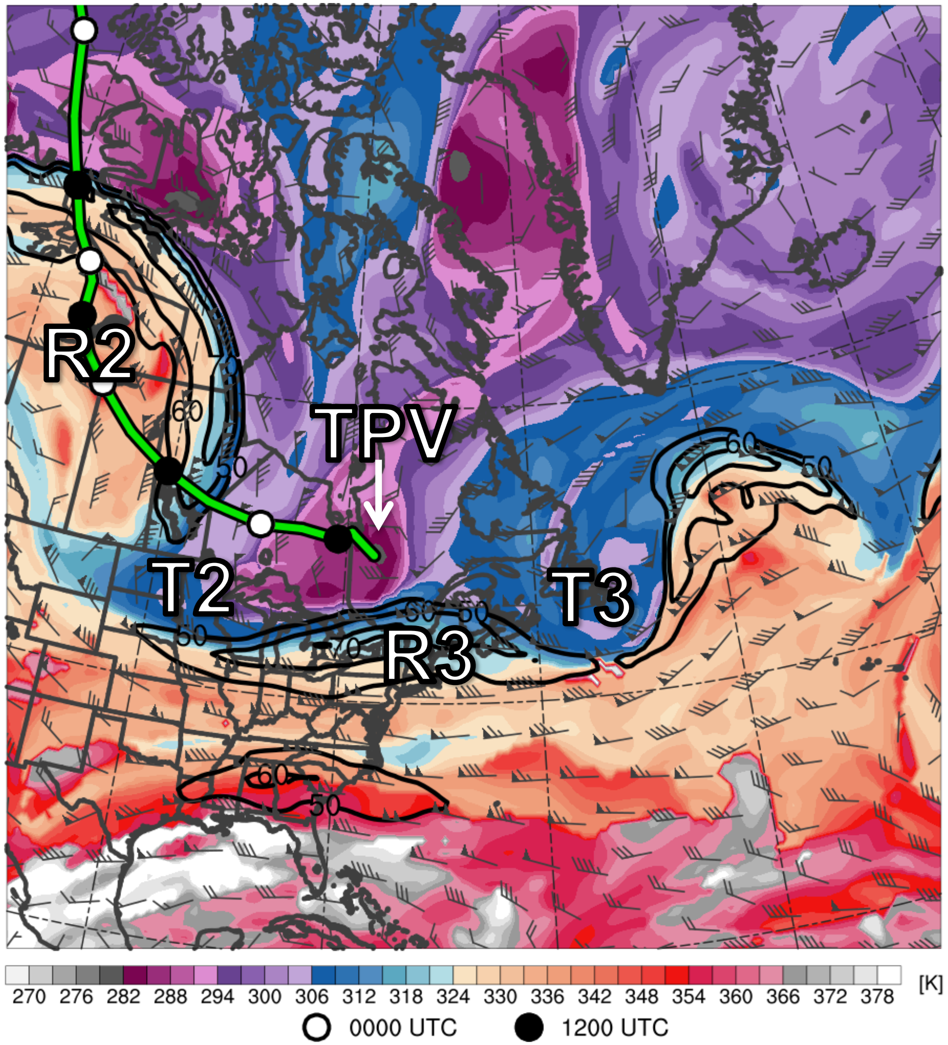

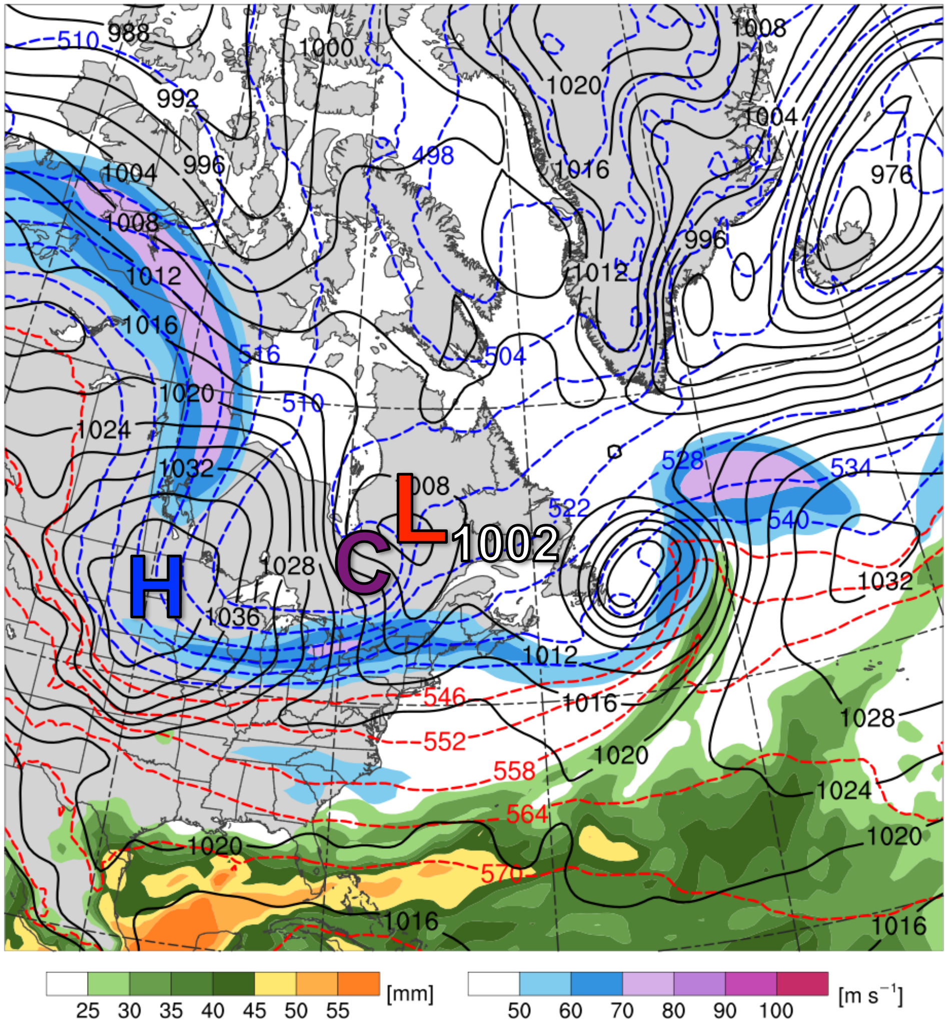

Potential temperature (K, shaded), wind speed (black, every 10 m s^{-1} starting at 50 m s^{-1}), and wind (m s^{-1}, barbs) on 2-PVU surface	250-hPa wind speed (m s^{-1}, shaded), 1000–500-hPa thickness (dam, blue/red), MSLP (hPa, black), PW (mm, shaded)

TPV–NAJ Interaction

1200 UTC 12 Nov 2013

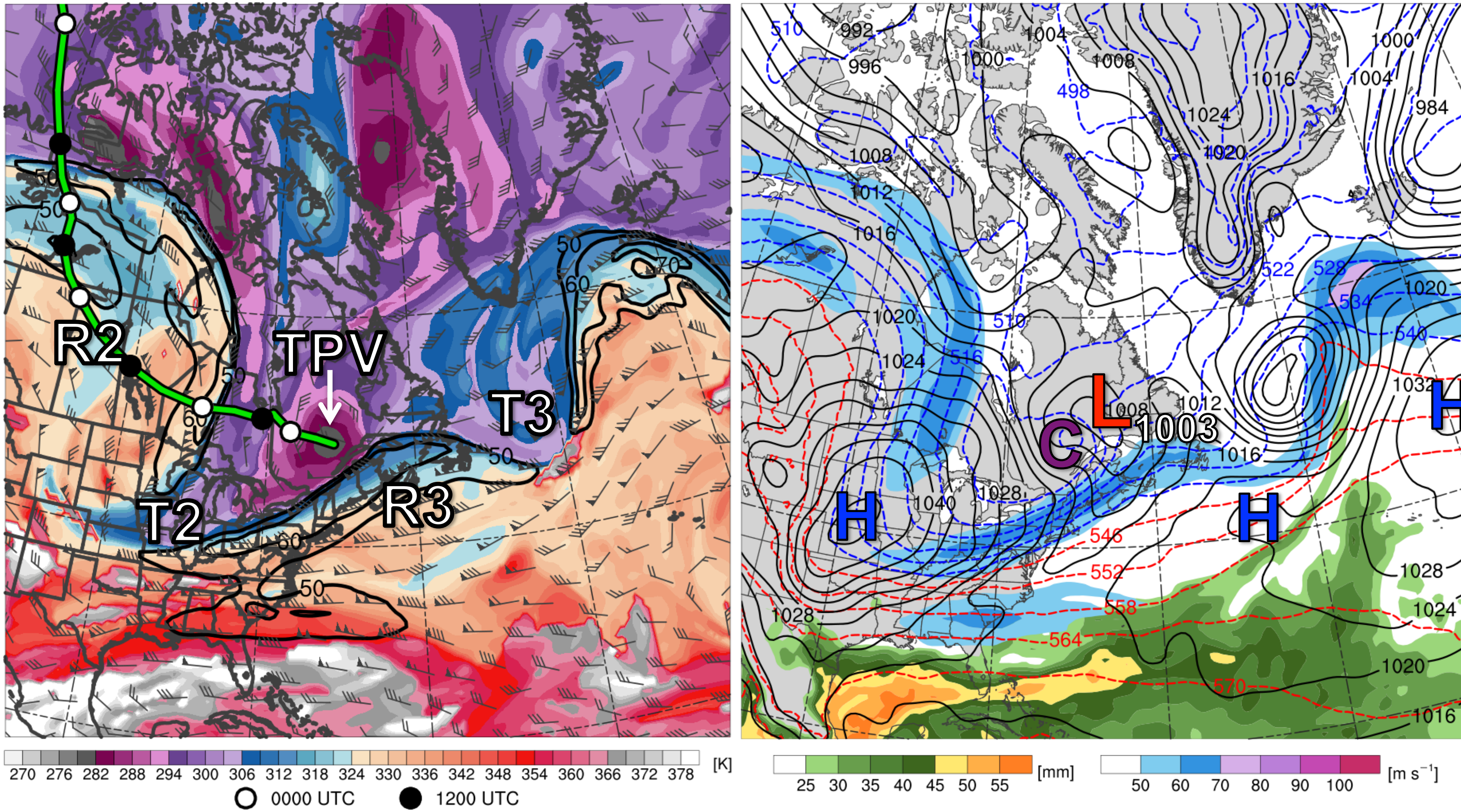

Potential temperature (K, shaded), wind speed (black, every 10 m s^{-1} starting at 50 m s^{-1}), and wind (m s^{-1}, barbs) on 2-PVU surface

250-hPa wind speed (m s^{-1}, shaded), 1000–500-hPa thickness (dam, blue/red), MSLP (hPa, black), PW (mm, shaded)

TPV–NAJ Interaction

0000 UTC 13 Nov 2013

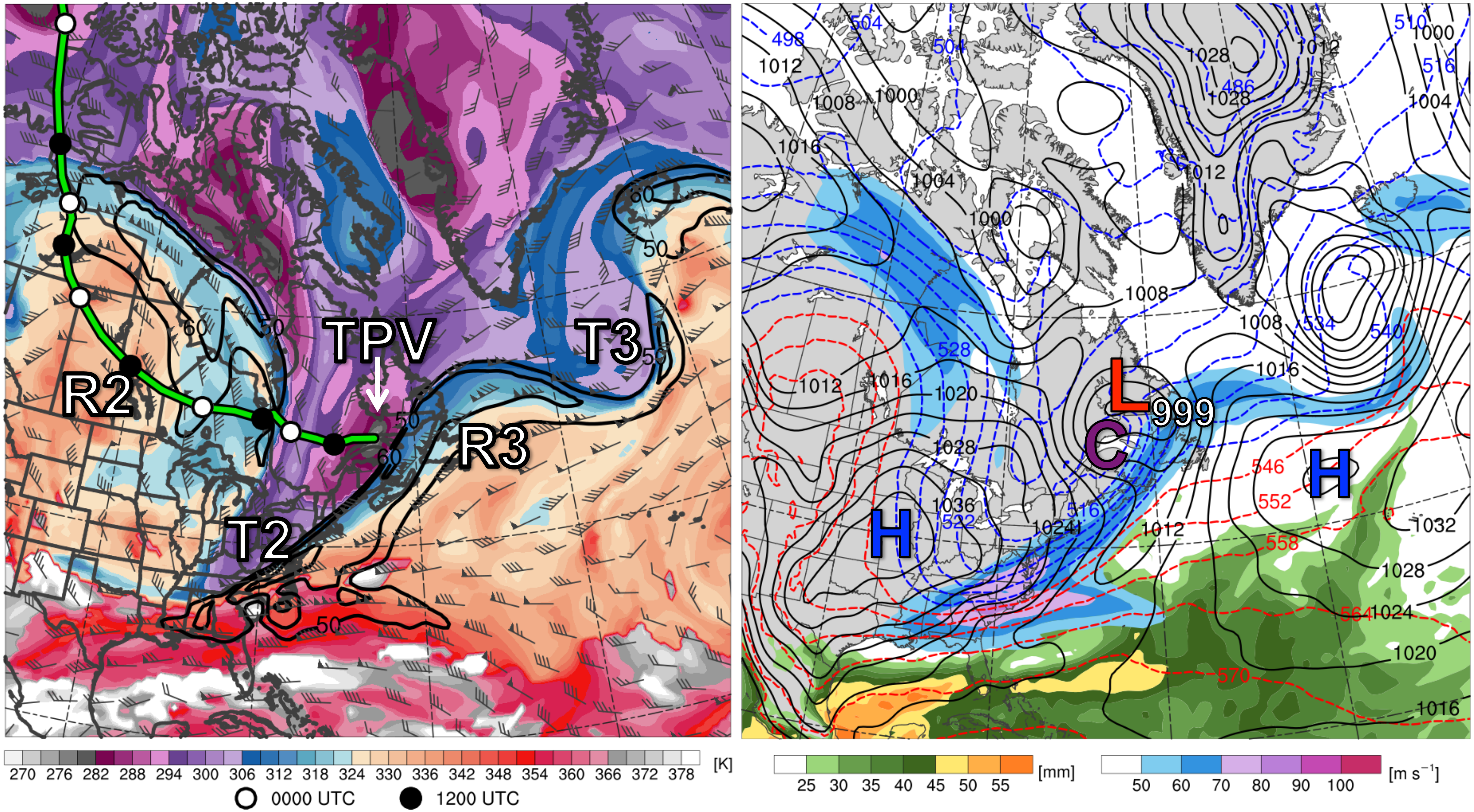

Potential temperature (K, shaded), wind speed (black, every 10 m s^{-1} starting at 50 m s^{-1}), and wind (m s^{-1}, barbs) on 2-PVU surface

250-hPa wind speed (m s^{-1}, shaded), 1000–500-hPa thickness (dam, blue/red), MSLP (hPa, black), PW (mm, shaded)

TPV–NAJ Interaction

1200 UTC 13 Nov 2013

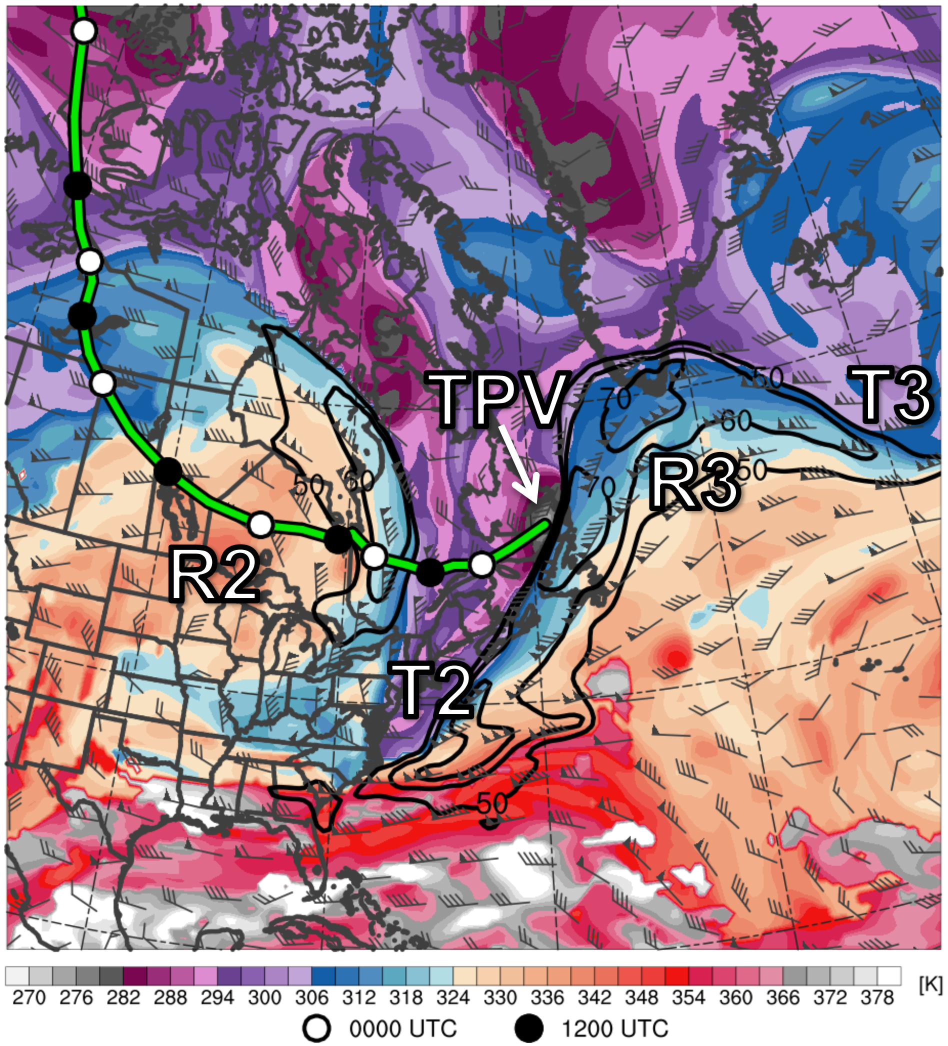

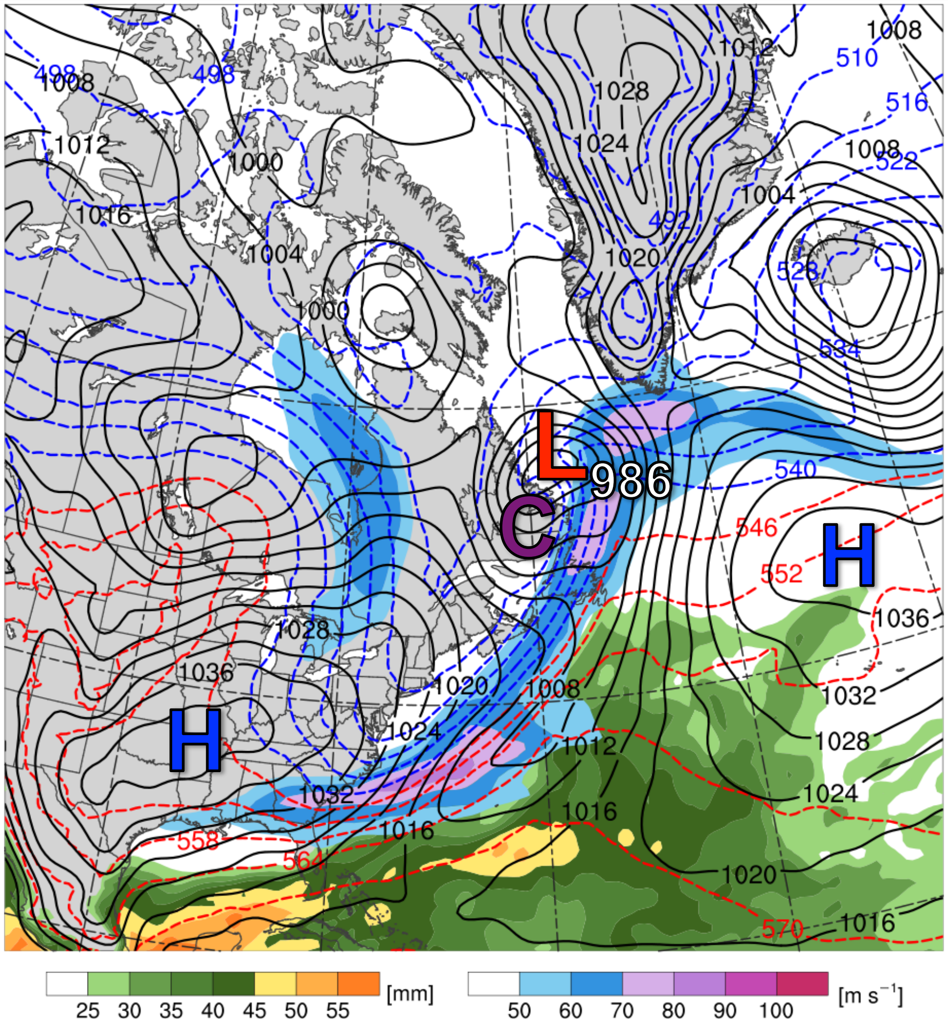

Potential temperature (K, shaded), wind speed (black, every 10 m s^{-1} starting at 50 m s^{-1}), and wind (m s^{-1}, barbs) on 2-PVU surface	250-hPa wind speed (m s^{-1}, shaded), 1000–500-hPa thickness (dam, blue/red), MSLP (hPa, black), PW (mm, shaded)

TPV–NAJ Interaction

1200 UTC 13 Nov 2013

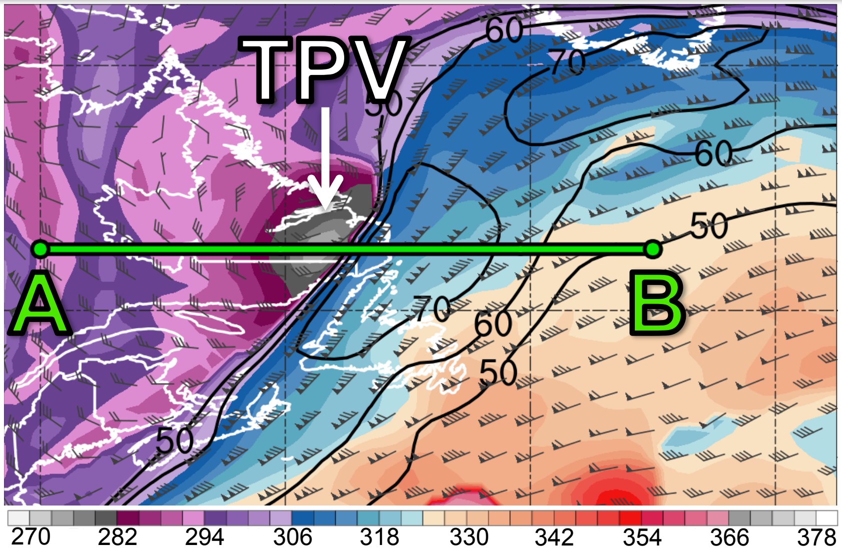

DT potential temperature (K, shaded), wind speed (black, every 10 m s^{-1} starting at 50 m s^{-1}), and wind (m s^{-1}, barbs)

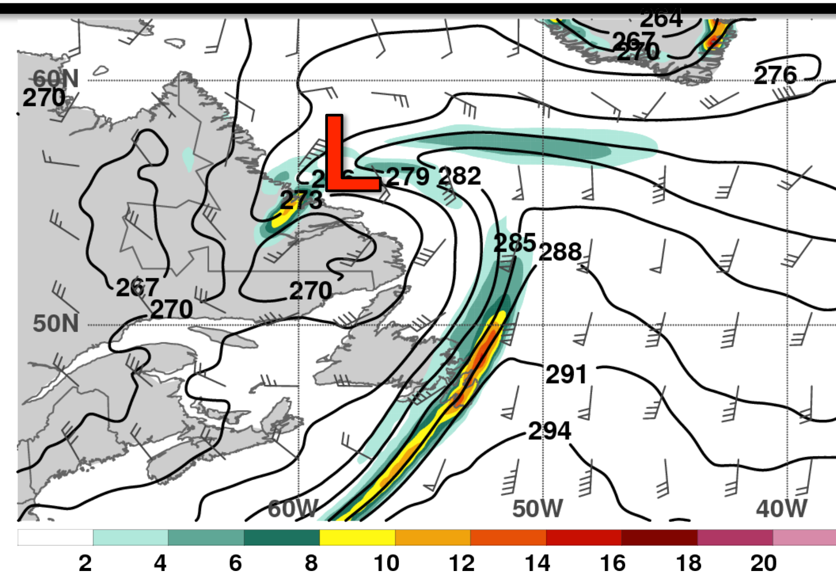

925–850-hPa θ (K, black), frontogenesis due to full horizontal wind [K (100 km)$^{-1}$ (3 h)$^{-1}$, shaded], and wind (m s^{-1}, barbs)

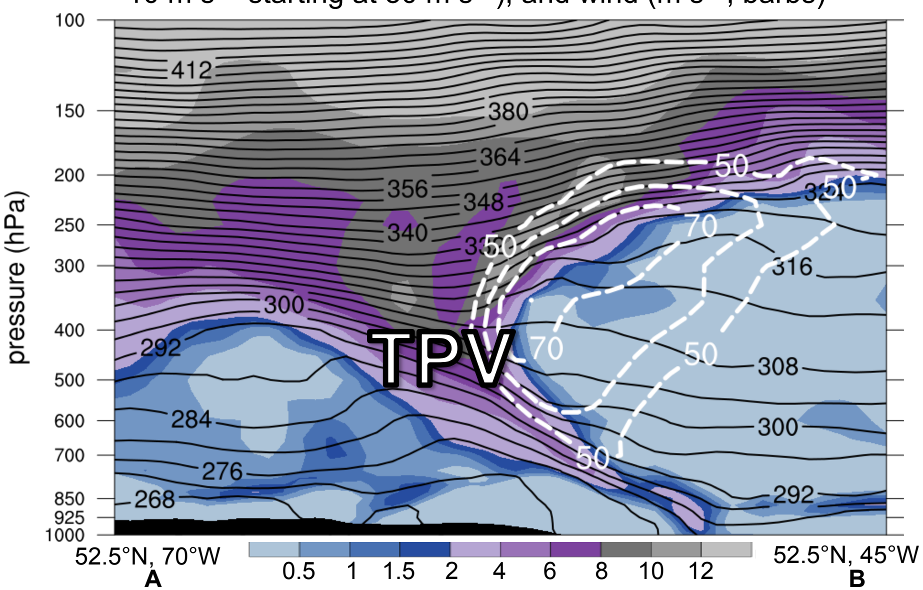

Potential vorticity (PVU, shaded), wind speed (white, every 10 m s^{-1} starting at 50 m s^{-1}), and potential temperature (K, black)

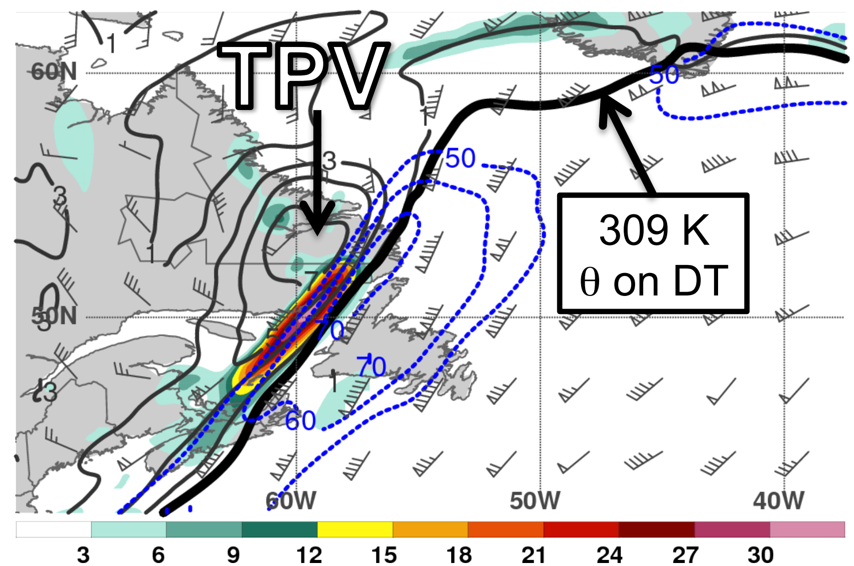

450–350-hPa PV (PVU, gray), PV frontogenesis due to full horizontal wind [PVU (100 km)$^{-1}$ (day)$^{-1}$, shaded], wind speed (m s^{-1}, blue)

Downstream Development

0000 UTC 14 Nov 2013

300–200-hPa PV (PVU, gray) and irrot. wind (m s^{-1}, vectors), 250-hPa wind speed (m s^{-1}, shaded), 600–400-hPa ascent (every 0.5 × 10^{-3} hPa s^{-1}, red), PW (mm, shaded)

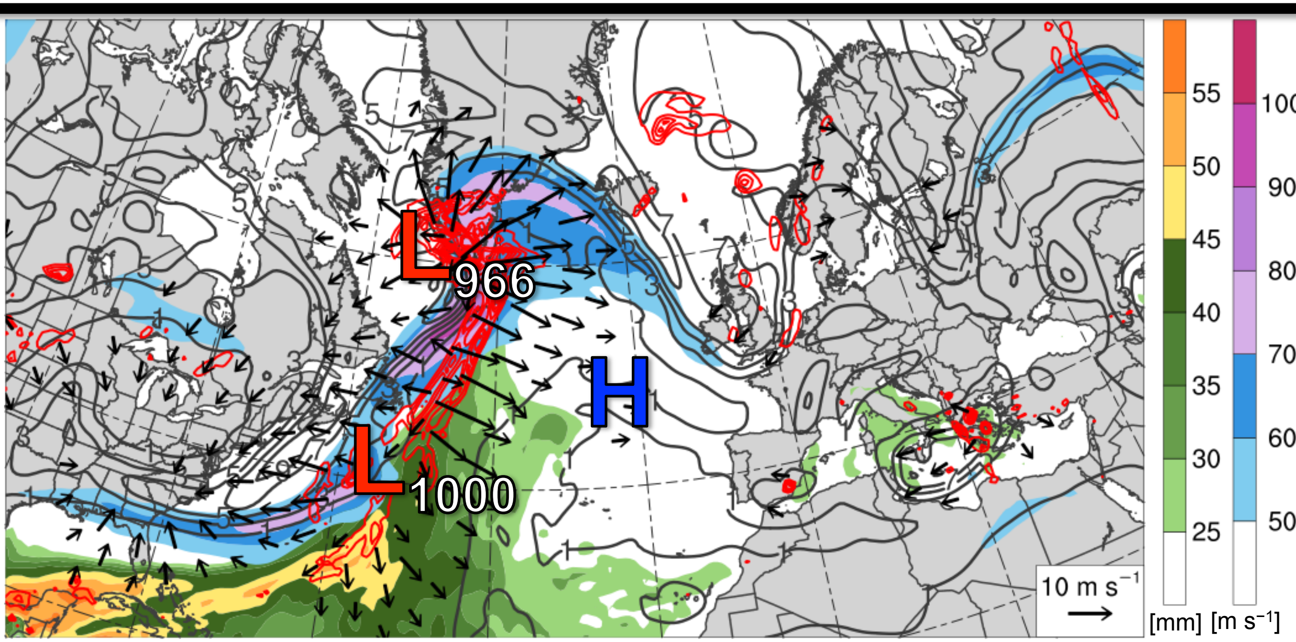

DT θ (K, shaded), wind speed (black, every 10 m s^{-1} starting at 50 m s^{-1}), and wind (m s^{-1}, barbs) on 2-PVU surface

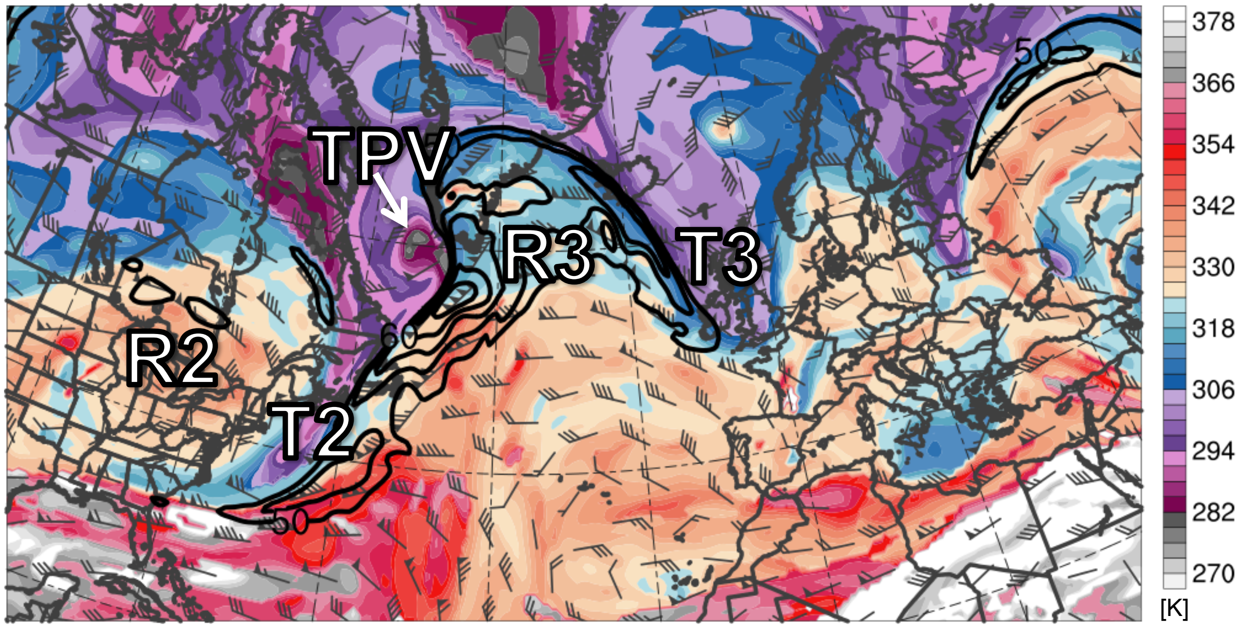

Downstream Development

1200 UTC 14 Nov 2013

300–200-hPa PV (PVU, gray) and irrot. wind (m s^{-1}, vectors), 250-hPa wind speed (m s^{-1}, shaded), 600–400-hPa ascent (every 0.5 × 10^{-3} hPa s^{-1}, red), PW (mm, shaded)

DT θ (K, shaded), wind speed (black, every 10 m s^{-1} starting at 50 m s^{-1}), and wind (m s^{-1}, barbs) on 2-PVU surface

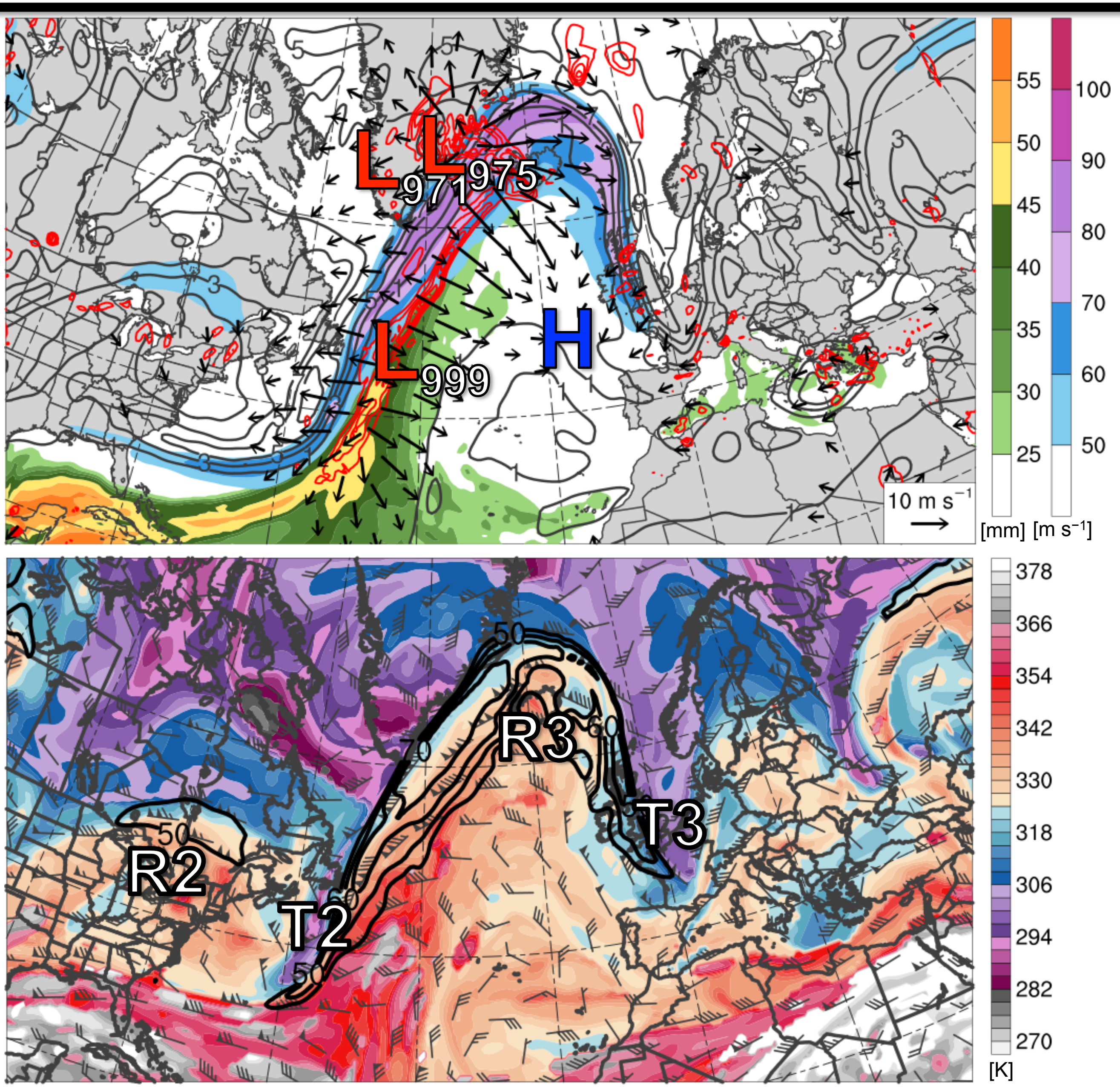

Downstream Development

0000 UTC 15 Nov 2013

300–200-hPa PV (PVU, gray) and irrot. wind (m s^{-1}, vectors), 250-hPa wind speed (m s^{-1}, shaded), 600–400-hPa ascent (every 0.5 × 10^{-3} hPa s^{-1}, red), PW (mm, shaded)

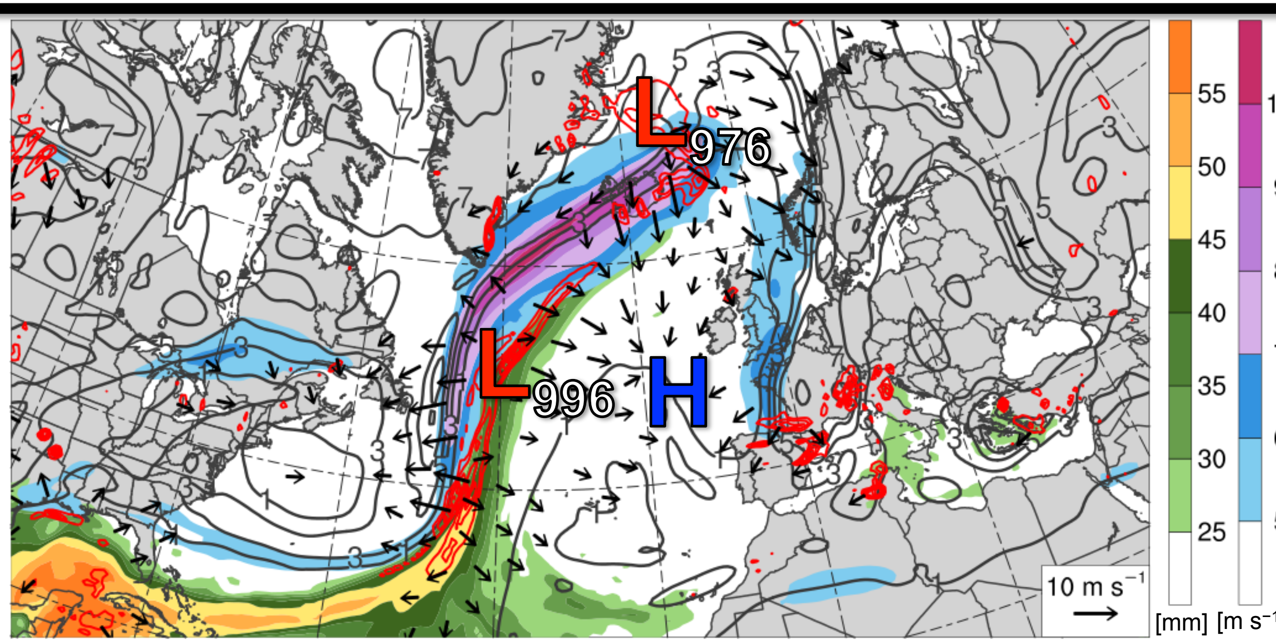

DT θ (K, shaded), wind speed (black, every 10 m s^{-1} starting at 50 m s^{-1}), and wind (m s^{-1}, barbs) on 2-PVU surface

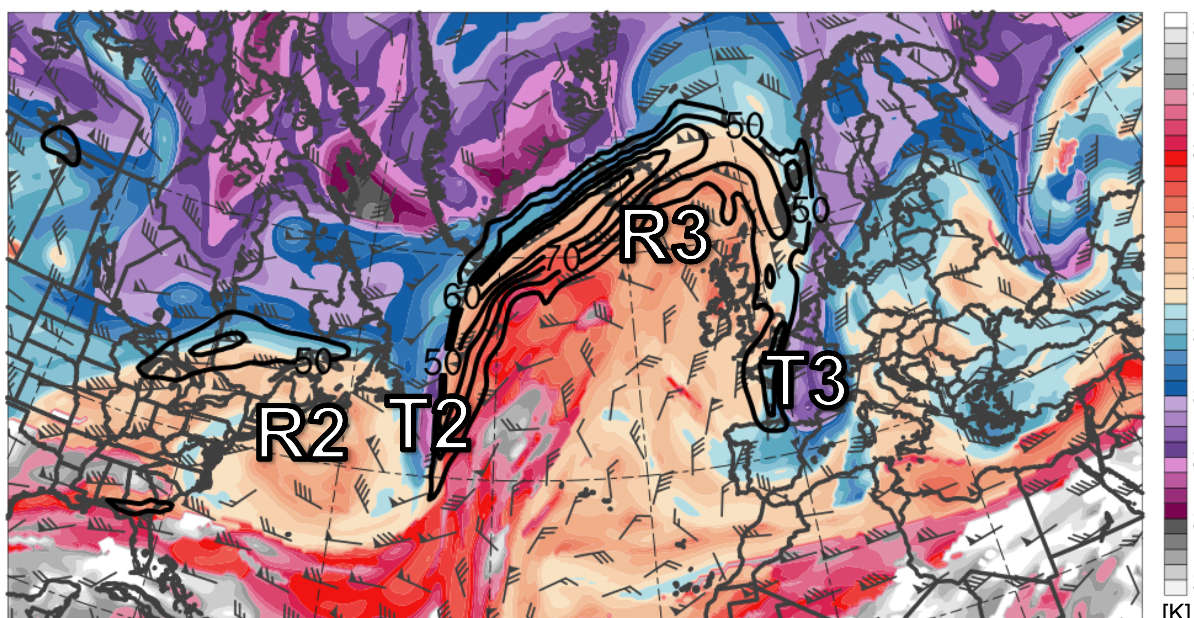

Downstream Development

1200 UTC 15 Nov 2013

300–200-hPa PV (PVU, gray) and irrot. wind (m s^{-1}, vectors), 250-hPa wind speed (m s^{-1}, shaded), 600–400-hPa ascent (every 0.5 × 10^{-3} hPa s^{-1}, red), PW (mm, shaded)

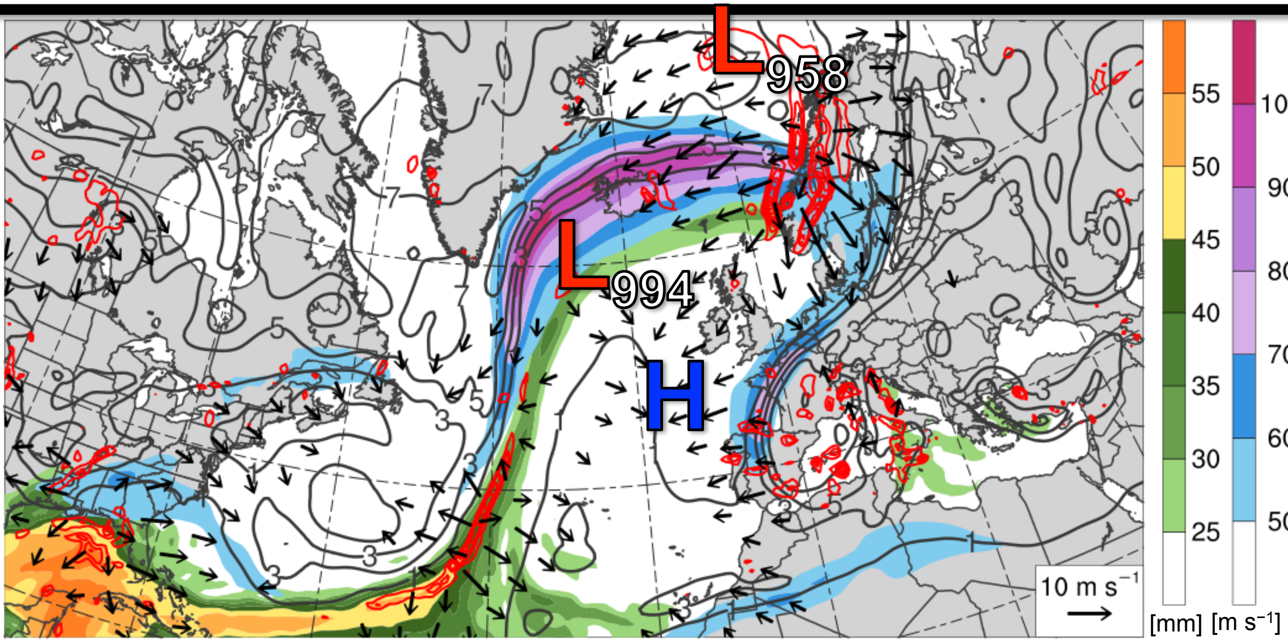

DT θ (K, shaded), wind speed (black, every 10 m s^{-1} starting at 50 m s^{-1}), and wind (m s^{-1}, barbs) on 2-PVU surface

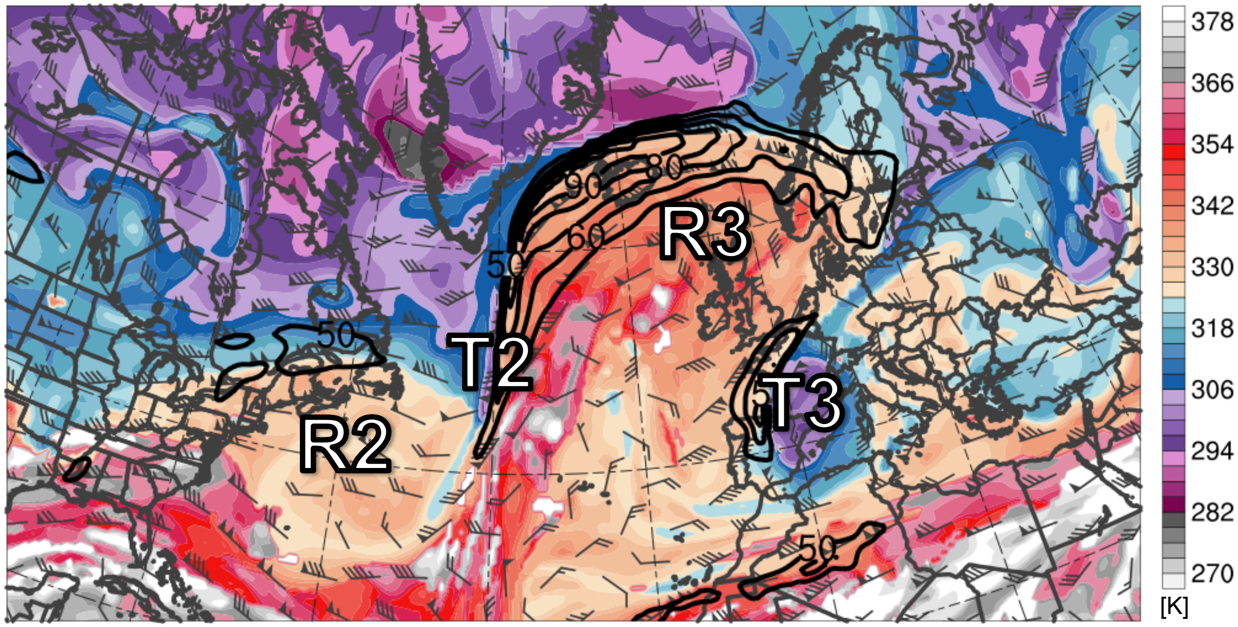

Downstream Development

0000 UTC 16 Nov 2013

300–200-hPa PV (PVU, gray) and irrot. wind (m s^{-1}, vectors), 250-hPa wind speed (m s^{-1}, shaded), 600–400-hPa ascent (every 0.5 × 10^{-3} hPa s^{-1}, red), PW (mm, shaded)

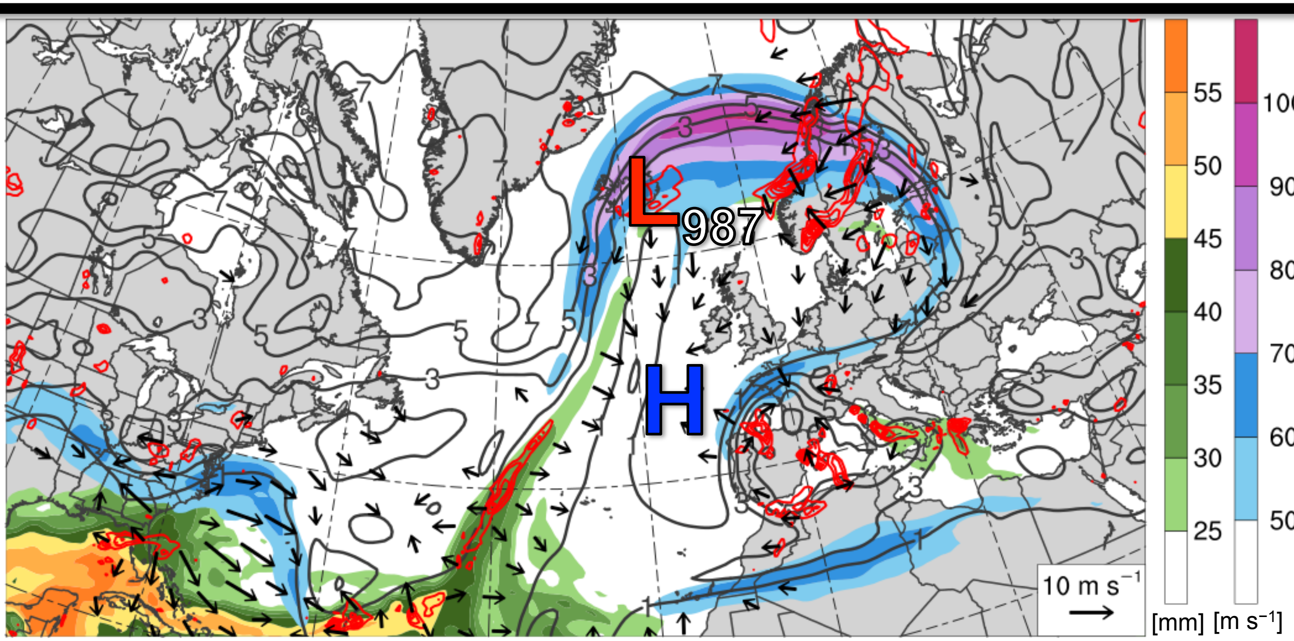

DT θ (K, shaded), wind speed (black, every 10 m s^{-1} starting at 50 m s^{-1}), and wind (m s^{-1}, barbs) on 2-PVU surface

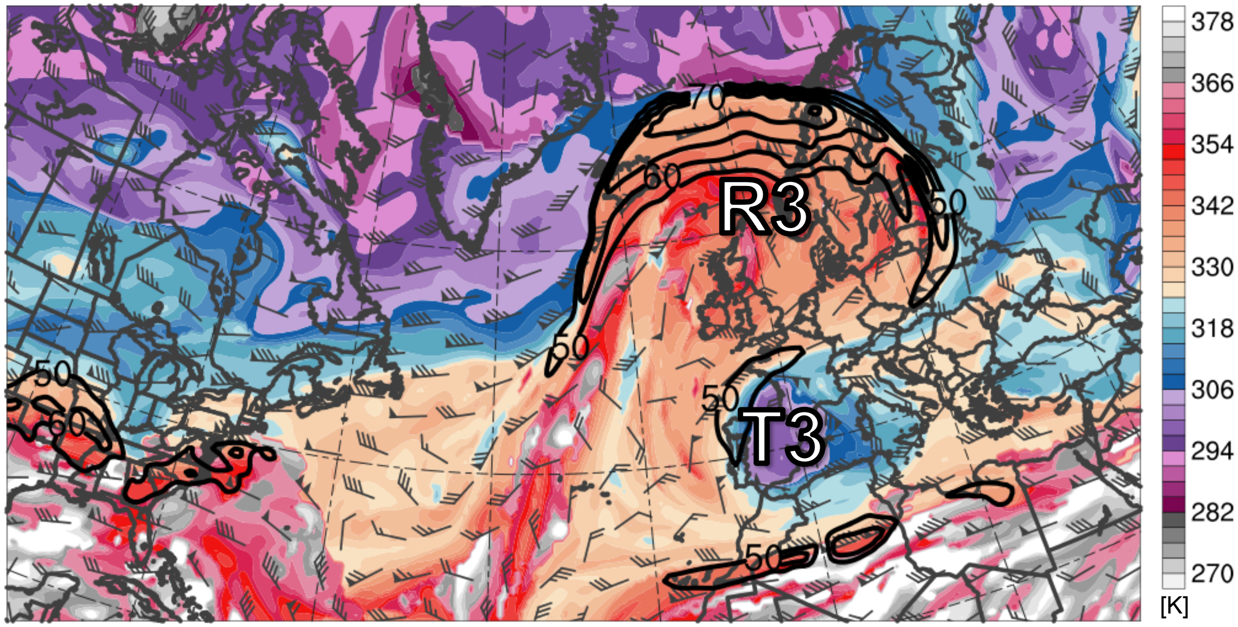

Downstream Development

1200 UTC 16 Nov 2013

300–200-hPa PV (PVU, gray) and irrot. wind (m s^{-1}, vectors), 250-hPa wind speed (m s^{-1}, shaded), 600–400-hPa ascent (every 0.5 × 10^{-3} hPa s^{-1}, red), PW (mm, shaded)

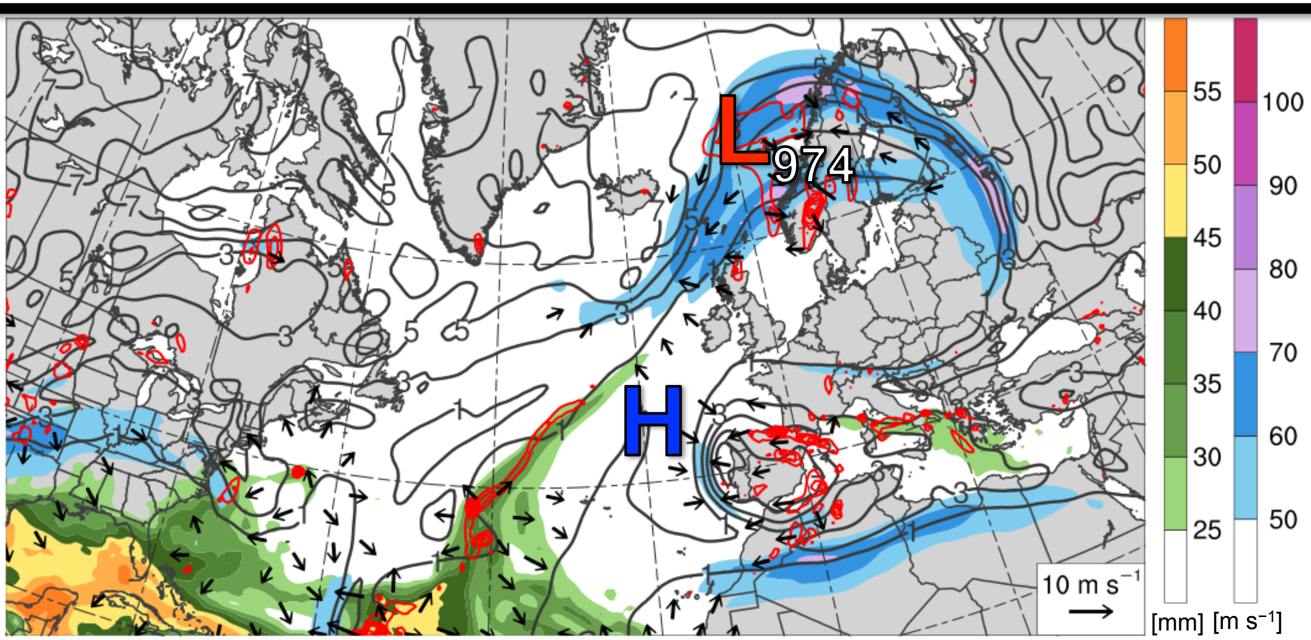

DT θ (K, shaded), wind speed (black, every 10 m s^{-1} starting at 50 m s^{-1}), and wind (m s^{-1}, barbs) on 2-PVU surface

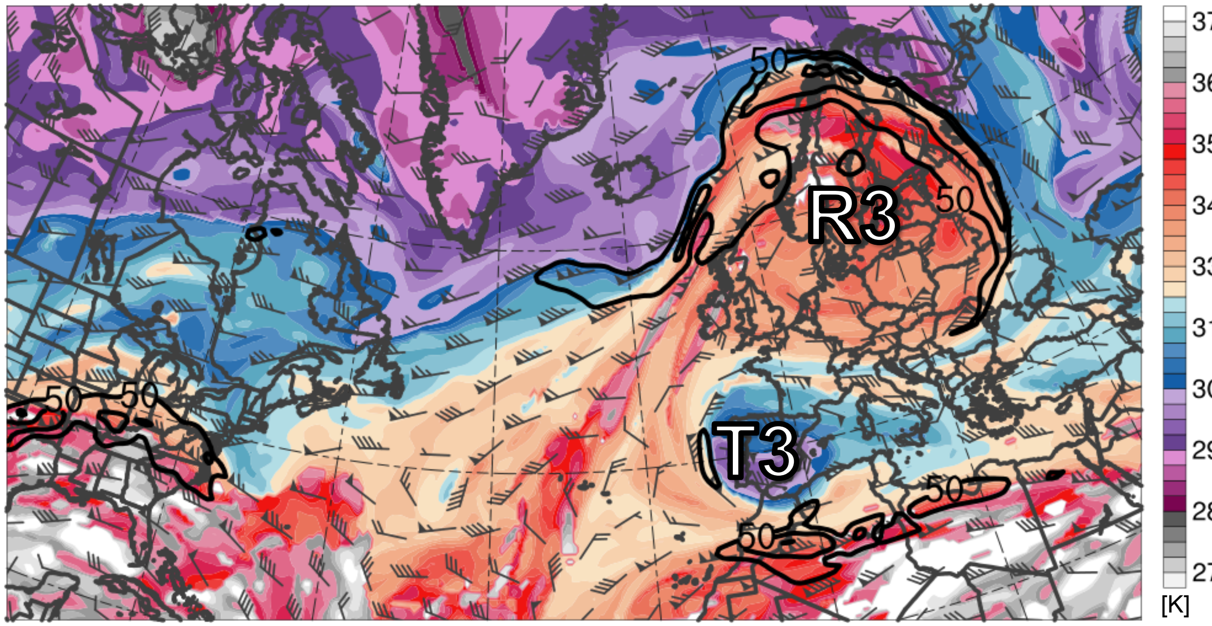

Downstream Development

0000 UTC 17 Nov 2013

300–200-hPa PV (PVU, gray) and irrot. wind (m s^{-1}, vectors), 250-hPa wind speed (m s^{-1}, shaded), 600–400-hPa ascent (every 0.5 × 10^{-3} hPa s^{-1}, red), PW (mm, shaded)

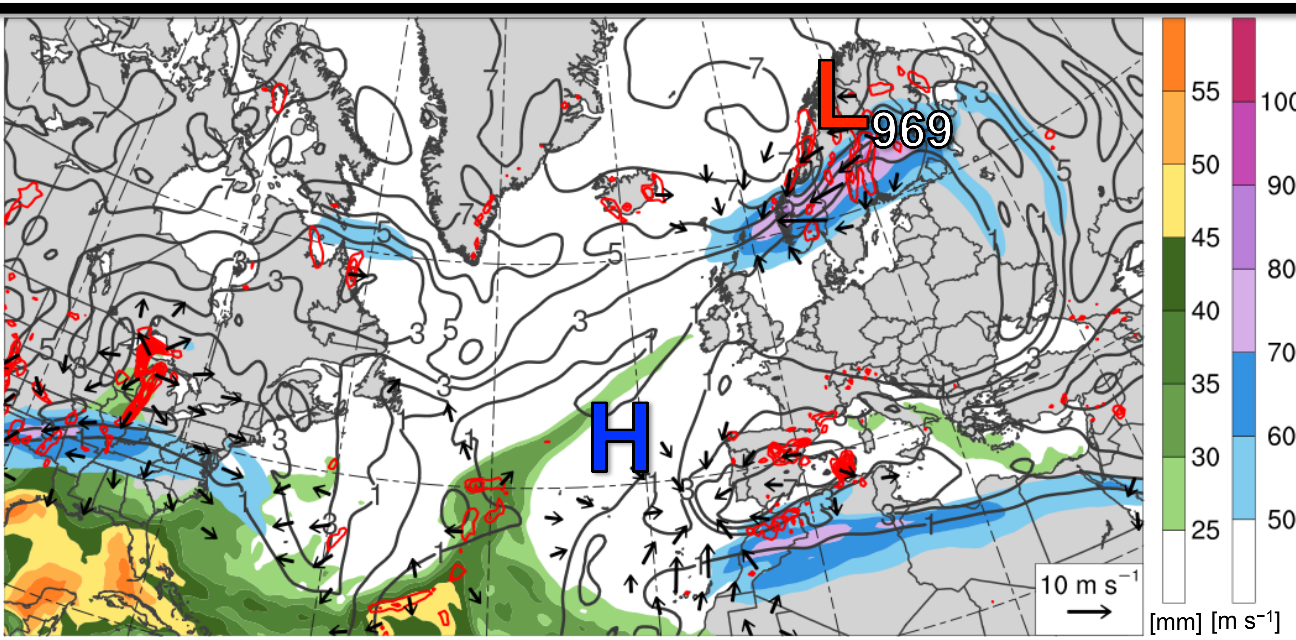

DT θ (K, shaded), wind speed (black, every 10 m s^{-1} starting at 50 m s^{-1}), and wind (m s^{-1}, barbs) on 2-PVU surface

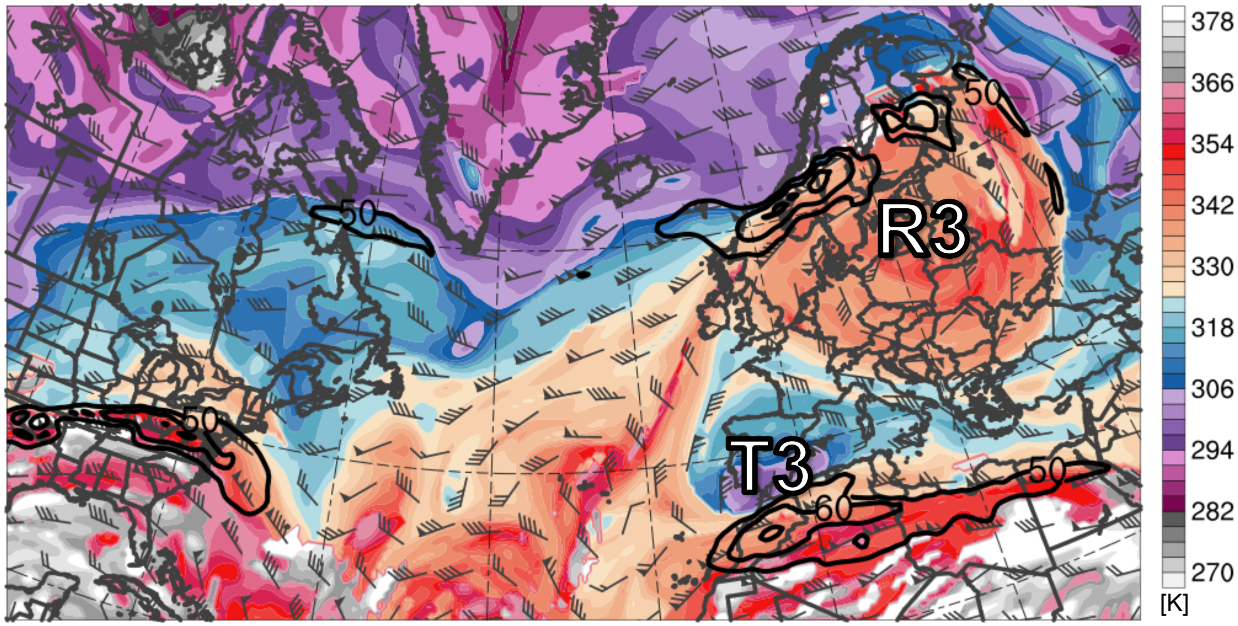

Downstream Development

1200 UTC 17 Nov 2013

300–200-hPa PV (PVU, gray) and irrot. wind (m s^{-1}, vectors), 250-hPa wind speed (m s^{-1}, shaded), 600–400-hPa ascent (every 0.5 × 10^{-3} hPa s^{-1}, red), PW (mm, shaded)

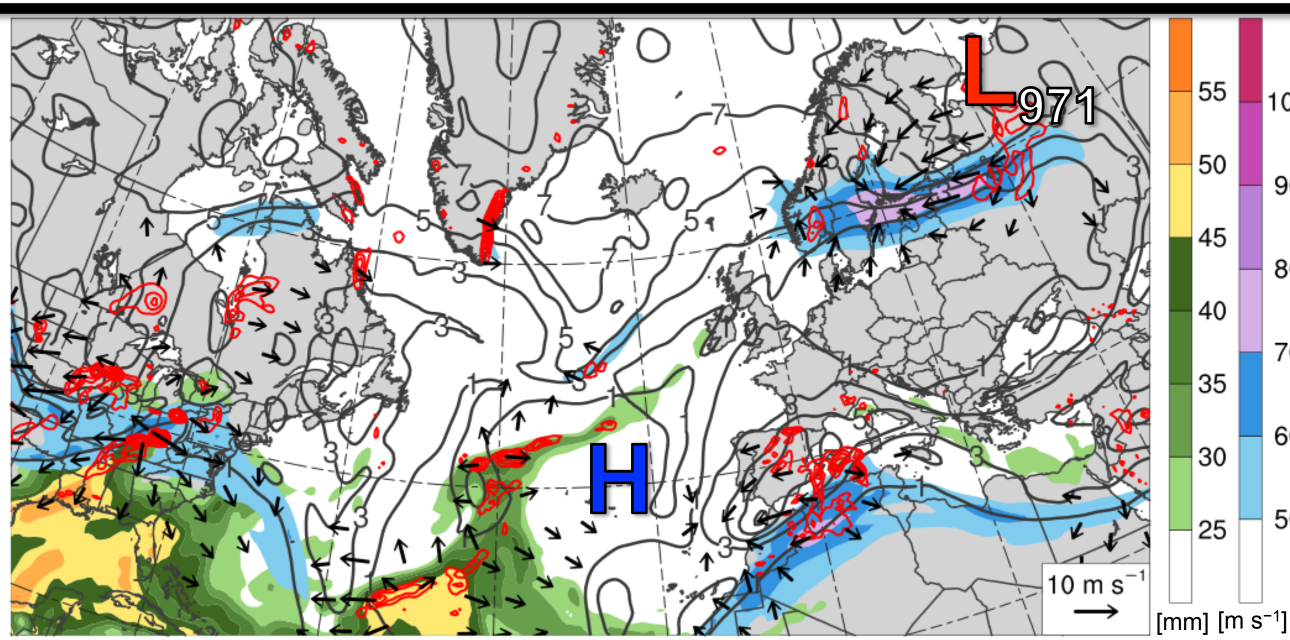

DT θ (K, shaded), wind speed (black, every 10 m s^{-1} starting at 50 m s^{-1}), and wind (m s^{-1}, barbs) on 2-PVU surface

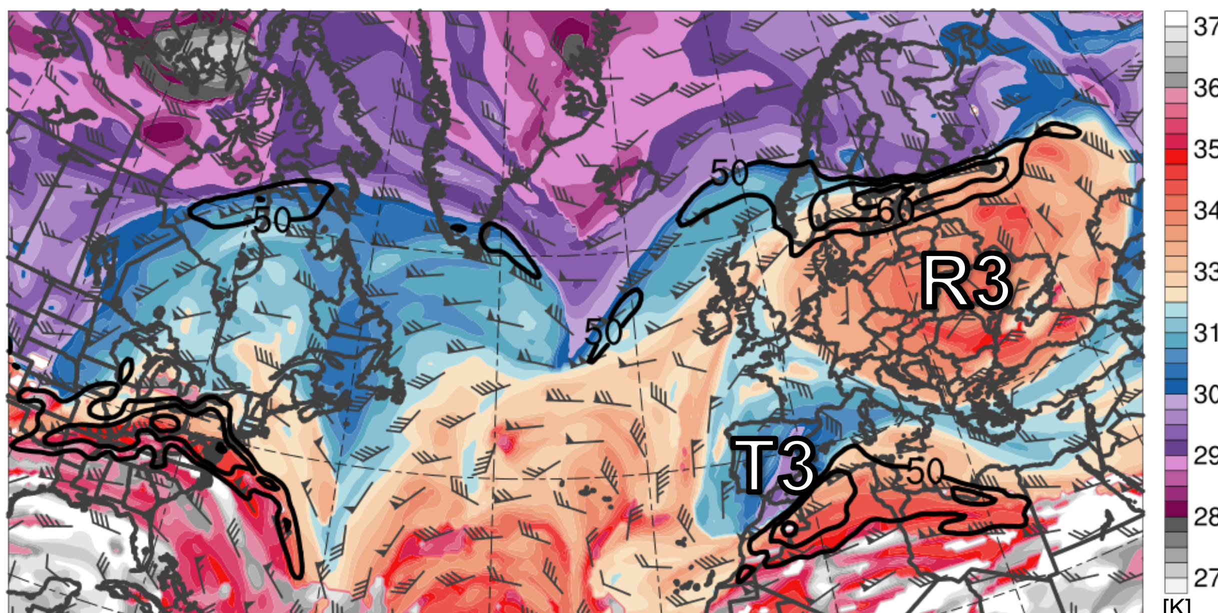

Downstream Development

0000 UTC 18 Nov 2013

300–200-hPa PV (PVU, gray) and irrot. wind (m s^{-1}, vectors), 250-hPa wind speed (m s^{-1}, shaded), 600–400-hPa ascent (every 0.5 × 10^{-3} hPa s^{-1}, red), PW (mm, shaded)

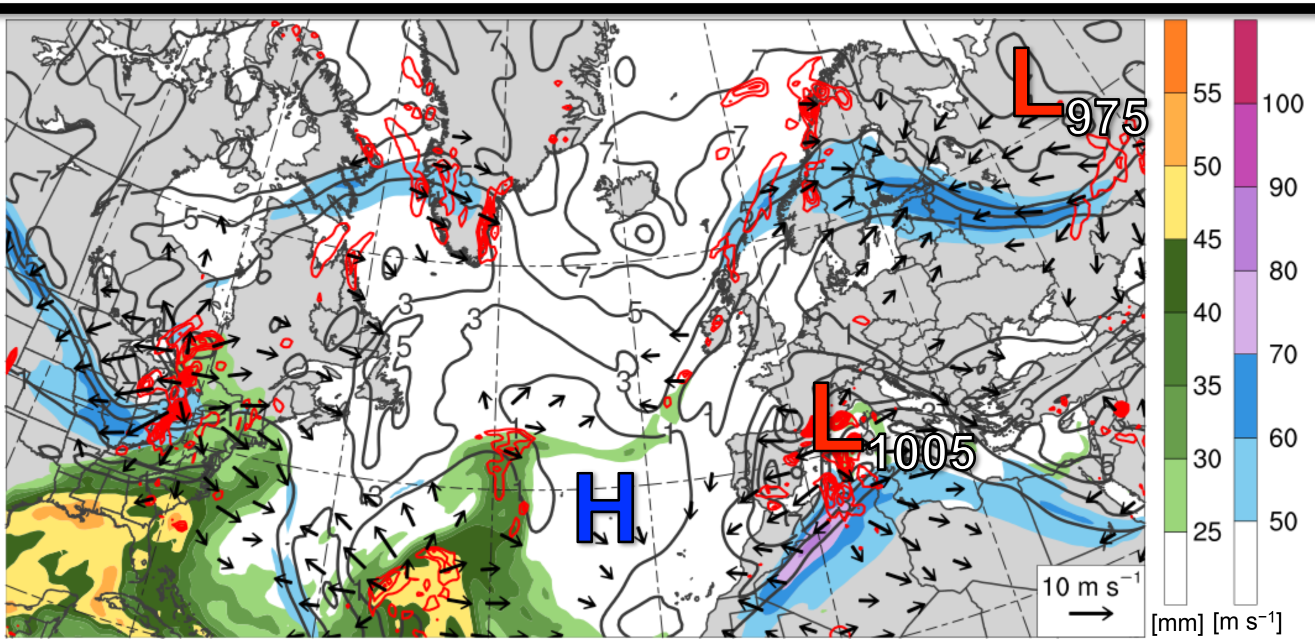

DT θ (K, shaded), wind speed (black, every 10 m s^{-1} starting at 50 m s^{-1}), and wind (m s^{-1}, barbs) on 2-PVU surface

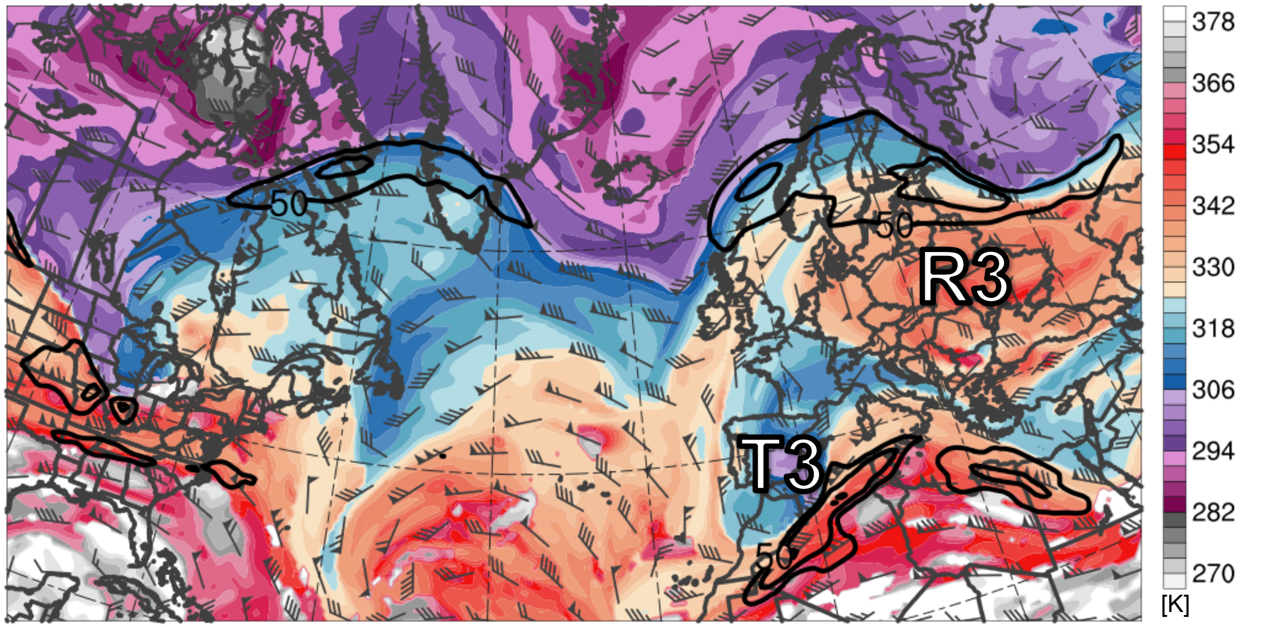

Downstream Development

1200 UTC 18 Nov 2013

300–200-hPa PV (PVU, gray) and irrot. wind (m s^{-1}, vectors), 250-hPa wind speed (m s^{-1}, shaded), 600–400-hPa ascent (every 0.5 × 10^{-3} hPa s^{-1}, red), PW (mm, shaded)

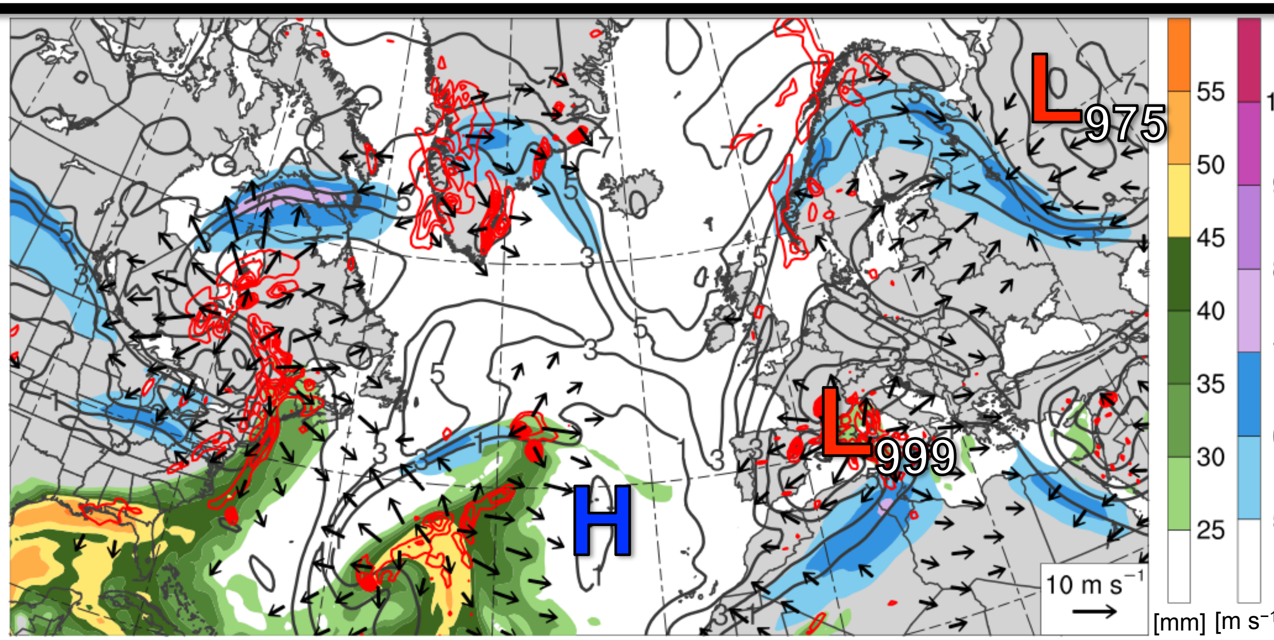

DT θ (K, shaded), wind speed (black, every 10 m s^{-1} starting at 50 m s^{-1}), and wind (m s^{-1}, barbs) on 2-PVU surface

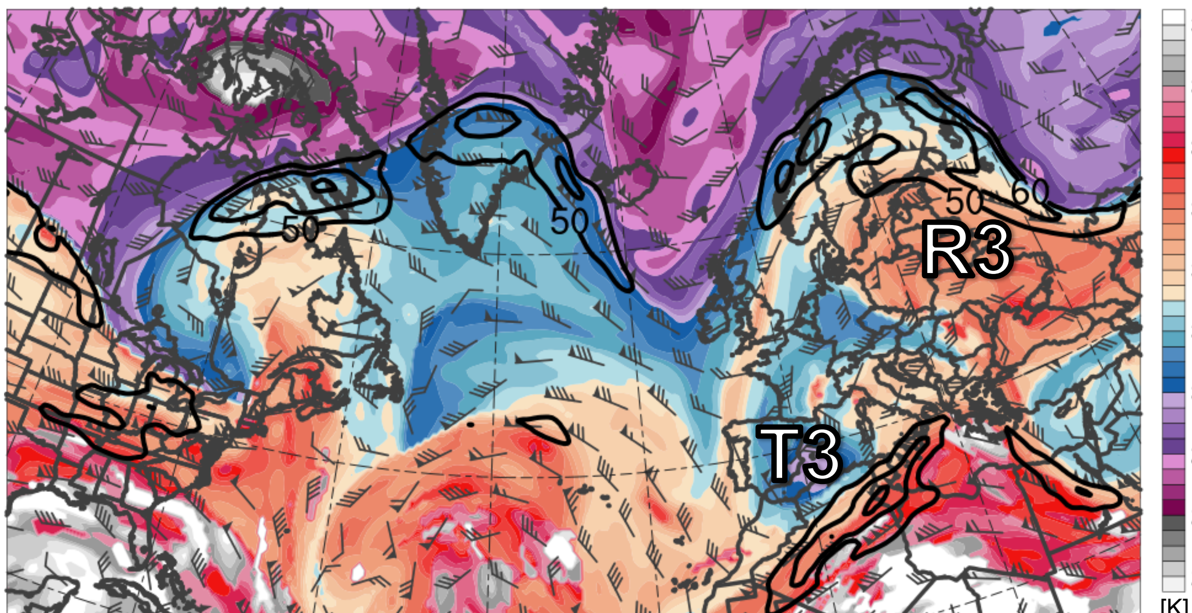

Flooding Event

1200 UTC 18 Nov 2013

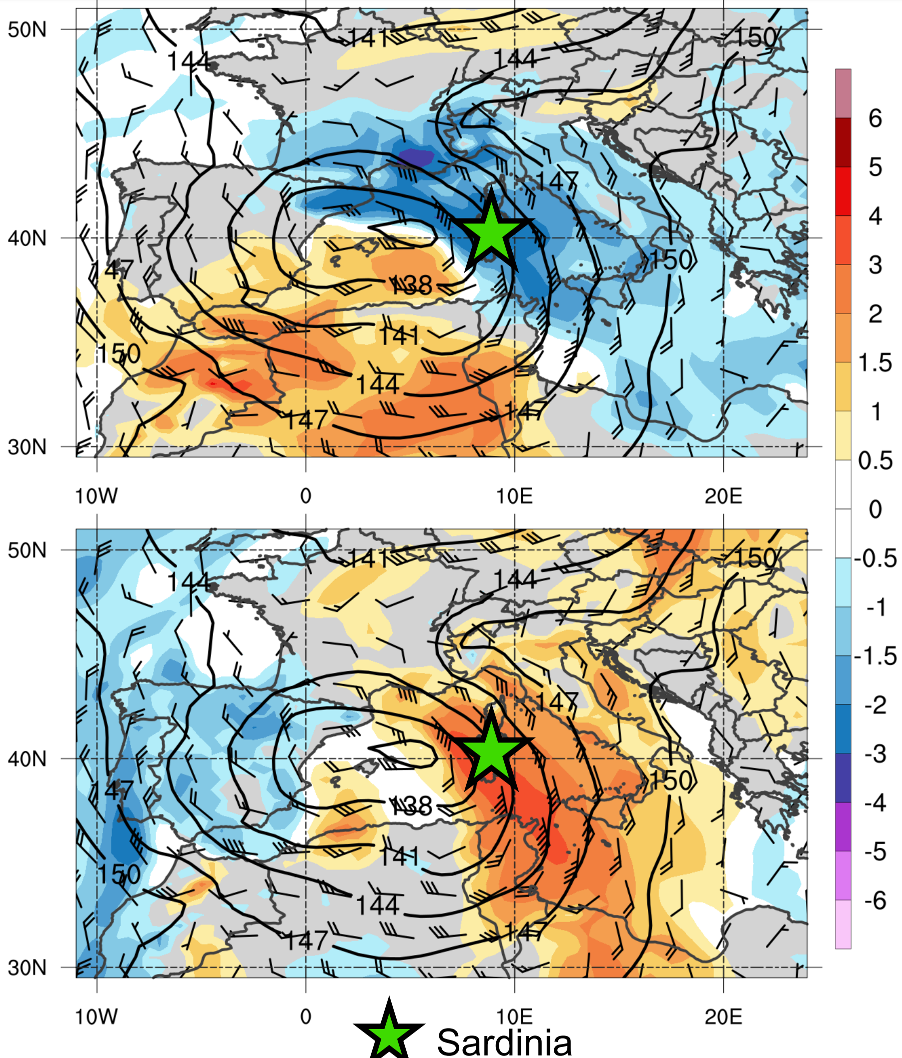

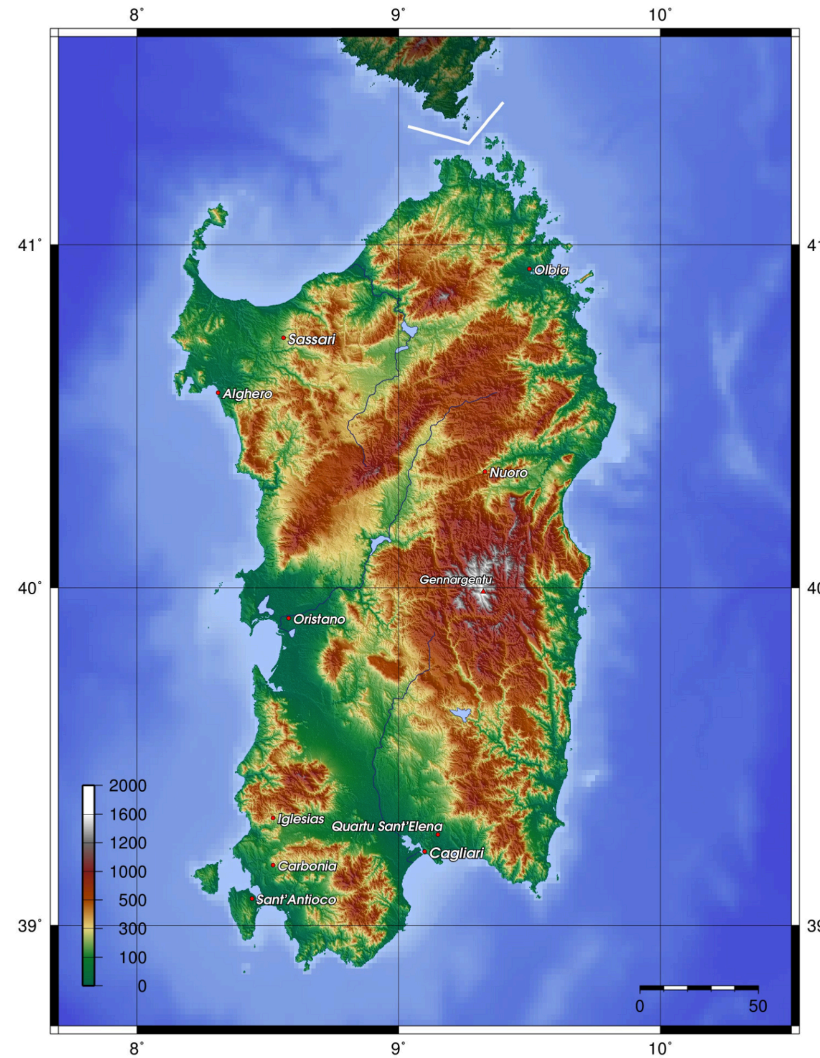

850-hPa geopotential height (dam, black), wind (m s^{-1}, barbs), and standardized anomalies (σ, shaded) of u wind (top) and v wind (bottom)

Relief map of Sardinia (Source: http://it.wikipedia.org/wiki/Campidano)

Flooding Event

1200 UTC 18 Nov 2013

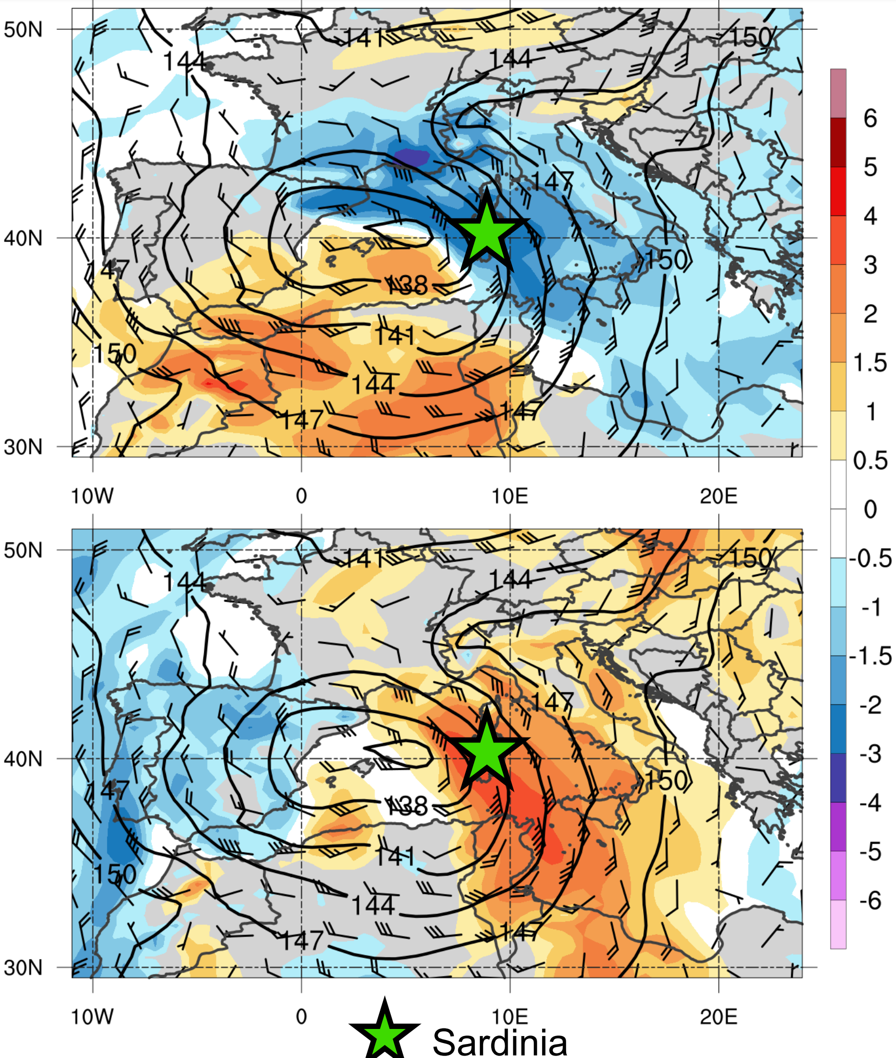

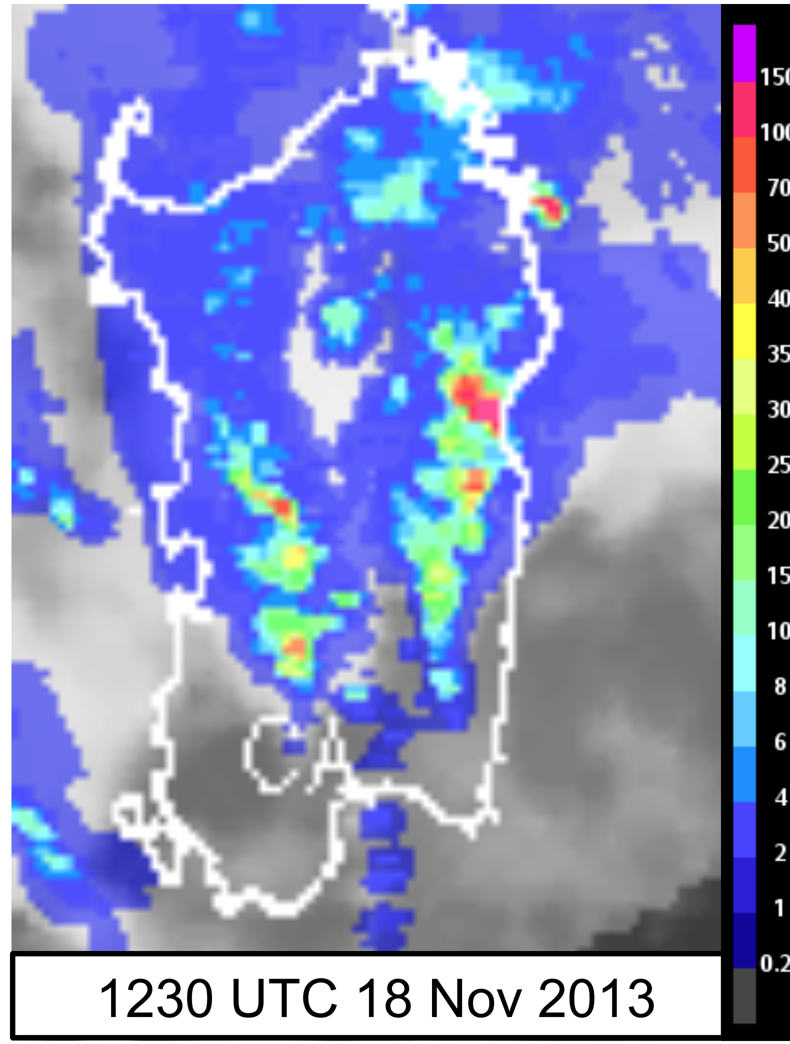

850-hPa geopotential height (dam, black), wind (m s^{-1}, barbs), and standardized anomalies (σ, shaded) of u wind (top) and v wind (bottom)

Radar-derived rainfall rate (mm h^{-1}, color shading) and IR brightness temperature (gray shading) valid 1230 UTC 18 Nov 2013 (Source: http://sop.hymex.org/)

Flooding Event

1200 UTC 18 Nov 2013

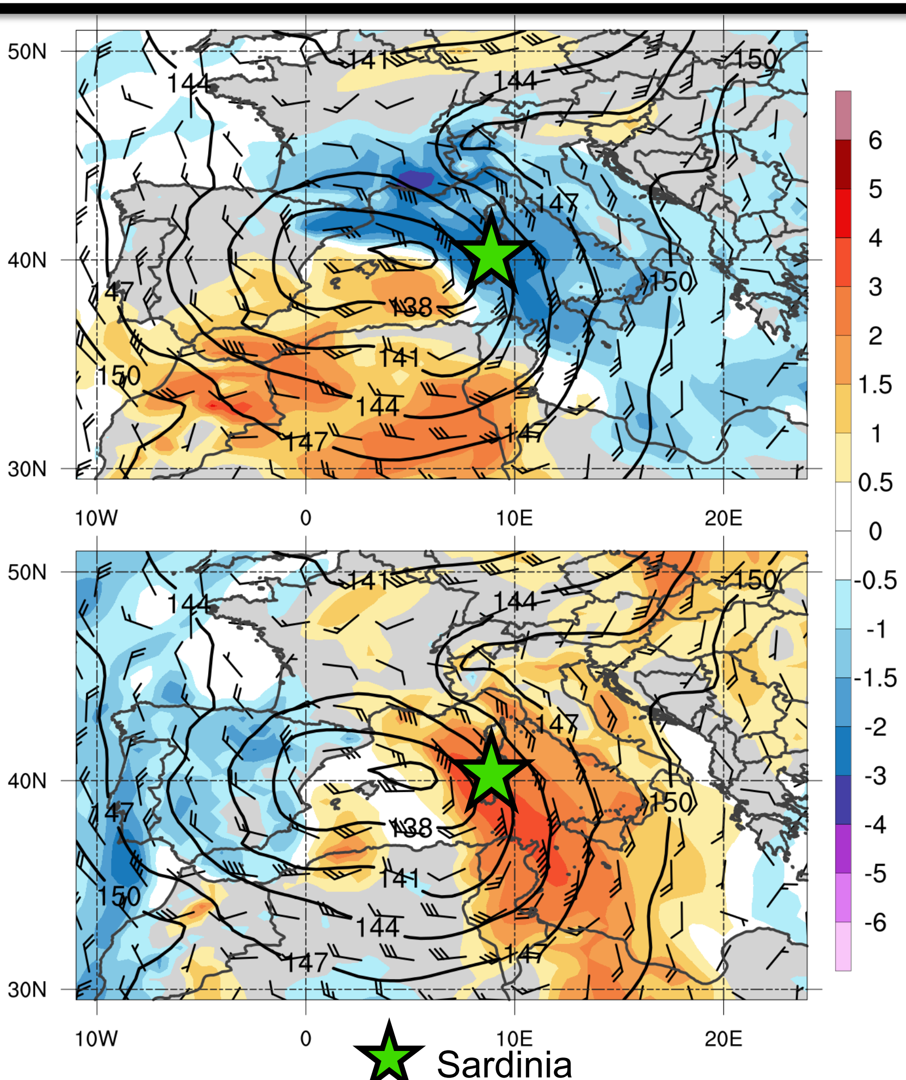

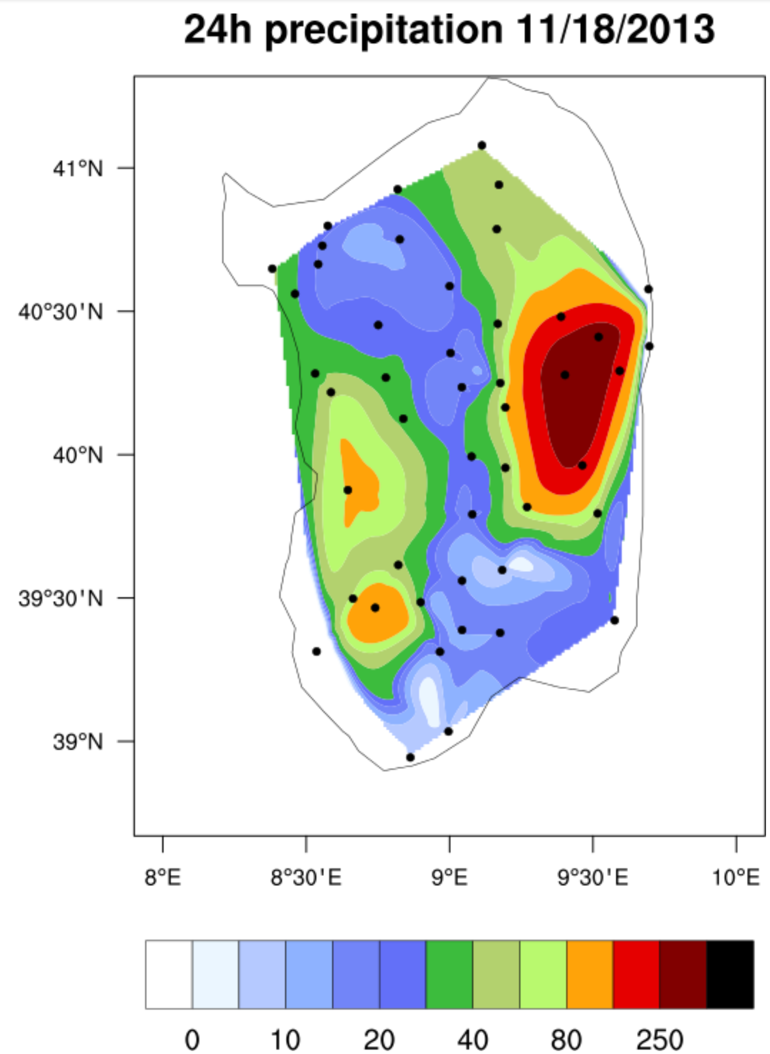

850-hPa geopotential height (dam, black), wind (m s^{-1}, barbs), and standardized anomalies (σ, shaded) of u wind (top) and v wind (bottom)

24-h accumulated precipitation (mm, shaded) during 18 Nov 2013 (Source: Julian Quinting)

Case Summary

- Explosive cyclogenesis over North Pacific leads to high-latitude ridge amplification
- Ridge amplification over North Pacific is critical to the extraction of TPV from high latitudes
- TPV and associated cold surge increase baroclinicity associated with NAJ throughout the troposphere
- Interaction between TPV and NAJ leads to explosive cyclogenesis in left-exit region of NAJ

Case Summary

- Interaction between TPV, upstream trough, and downstream anticyclone induce significant ridge amplification over western North Atlantic
- NAJ intensifies to over 100 m s^{-1} and wave breaks anticyclonically over northern Europe
- Downstream trough cuts off and retrogrades over southwestern Europe before interacting with subtropical jet over northern Africa
- Slow-moving cutoff cyclone over Mediterranean leads to anomalously strong southeasterly upslope flow and heavy rainfall over Sardinia